ONIUM PHYSICS AND SUPERSYMMETRY*

By J. H. KÜHN**

CERN — Geneva

(Received March 21, 1985)

After a brief review of the standard model's prediction for toponium, various consequences of supersymmetry on toponium S- and P-state decays are discussed. Depending on the mass of scalar quarks and gluinos, supersymmetry could have minor effects on toponium decays or alter its properties completely. We then predict the properties and production mechanisms of onia which are specific to supersymmetry: squarkonia and gluino balls.

PACS numbers: 11.30.Pb, 12.35.Ht

1. Introduction

Despite heroic efforts to push the energy of e^+e^- storage rings up to a centre-of-mass energy of 46.78 GeV, no sign of toponium or open top was found in e^+e^- annihilation. A lower limit on the mass of toponium of 46.78 GeV [1] has recently been reported, and similarly the threshold for open top production has been shown [1] to lie above 46 GeV[1].

This may seem somewhat disappointing, but the perspective for testing the conventional pattern of interactions or for finding new physics in toponium decays is becoming increasingly exciting with increasing toponium mass.

The short-range part of the quark-antiquark potential will be explored down to a distance of less than 0.1 fm [2], and numerous predictions of perturbative QCD for two-, three-, and four-jet topologies should be tested quite accurately [7]. For a toponium state with its mass of more than 45 GeV, one furthermore expects a remarkable interplay between strong, electromagnetic, and weak decays. For sufficiently large masses their "natural" order may even be reversed [8–16]. In particular, weak decays of a single t-quark inside toponium (SQDs) will become increasingly important above 45 GeV and — for masses

* Lectures presented at the XXIV Cracow School of Theoretical Physics, Zakopane, Poland, June 6–19, 1984.

** Address: Max-Planck-Inst. für Phys. und Astrophys., Föhringer 6, Postfach 40 12 12, D-8000 München 40.

[1] Indications for open top production with a top mass of 40 ± 10 GeV have recently been found at the CERN proton-antiproton collider [2].

[2] For a discussion of these issues, see, for example, Refs. [3] to [6].

larger than 60 GeV — will even dominate the three-gluon mode. For $M_{t\bar{t}}$ close to m_{Z^0} the overwhelming decay modes will be those through the neutral current. In this region toponium would manifest itself mainly through the change in the total cross-section. Branching ratios and final-state topologies will be quite similar both on and off resonance.

Toponium decays should be an excellent place to look for and eventually discover new particles or new interactions. The smaller production rate in comparison with reactions on the Z^0 will certainly be a serious drawback. However, this should be compensated by the larger branching ratio of toponium into potentially interesting channels such as γ + Higgs or various supersymmetric particles (gluino pairs, squarks, photinos, etc.). This advantage is due to the fact that in Z decays many of these modes are of higher order compared with $Z \to f\bar{f}$, whereas in $(t\bar{t})$ decays they are of the same order as the leading conventional ones. In addition, a larger variety of quantum numbers (1^{--}, 0^{++}, 1^{++}, 2^{++}) is accessible in quarkonium physics, which might help to reach otherwise inaccessible channels.

In this review we will first present the standard scenario of toponium decays; however, this is rather sensitive to the precise value of $M_{t\bar{t}}$ and varies rapidly above 50 GeV. We shall argue that even this standard picture is remarkably rich in its structure and will deserve long and dedicated experimental effort. In particular we shall discuss in some detail how predictions of QCD can be tested, and how charged-current as well as neutral-current couplings of top quarks can be measured.

In the second part of these lectures we shall show how supersymmetry could make this scenario even more colourful. The pattern of toponium decays will then depend quite sensitively on the masses of m_t and of the various additional particles imposed by supersymmetry. In some cases only minute modifications will be induced; in others the standard picture will be completely changed; or, in some extreme cases, toponium would no longer exist as well-defined resonance.

Section 3 of these lectures is devoted to the onia of supersymmetry. We shall review the properties of squarkonia and discuss their (non-) appearance in e^+e^- annihilations. Finally, we shall present the properties of gluino-gluino bound states. We shall review their quantum numbers, their level spacing, and their most promising production mechanisms. In particular we shall show how the search for these states in radiative quarkonium decays will cover a range of gluino masses in an almost-independent way.

2. Standard toponium

2.1. Properties of the $^3S_1$ ground state

The salient features of the $^3S_1$ ground state[3] V have been frequently discussed in the literature [5–14]. (For recent reviews see, for example, Refs. [14] to [18].) The production rate is of course dependent on its electronic width and thus on the wave function at the origin. Together with the 1S–2S level spacing, this is the quantity most sensitive to the

[3] The (tt) ground state will be denoted further on by V, the radial excitations by V′.

unknown short-distance part of the potential. Once these two quantities will have been measured, the potential will be virtually fixed and the remaining properties of toponium can be predicted unambiguously.

We will simply expose this model dependence whenever necessary. Evidently the extreme choices of the Cornell potential [$V(r) = a/r + br$] or of Martin's potential [$V(r) = A + Br^{0.1}$] will lead to drastically different predictions for the electronic widths.

However, even various potentials, all of which correspond to the logarithmically softened $1/r$ dependence suggested by QCD, lead to results differing by more than a factor of 1.5 already for $M_V = 80$ GeV. Within this uncertainty the naive assumption of a constant $\Gamma_0 = \Gamma(1^1S_1 \underset{\gamma}{\to} e^+e^-) \simeq 5$ keV seems to work reasonably well and will be accepted in this section.

The cross-section on top of the resonance is given by

$$\sigma_{\text{top}} = [|v|^2 + |a|^2] \frac{9\pi}{2\alpha^2 \sqrt{2\pi}} \frac{\Gamma_0}{\delta W} \left[\left(\frac{2\delta W}{M_V} \right)^t + \varepsilon \right] \sigma(e^+e^- \underset{\gamma}{\to} \mu^+\mu^-) \tag{2.1}$$

where

$$t = 2\frac{\alpha}{\pi}\left[\ln \frac{M_V^2}{m_e^2} - 1\right], \quad \varepsilon = \frac{2\alpha}{\pi}\left(\frac{\pi^2}{6} - \frac{17}{36}\right) + \frac{13}{12} t,$$

$$v = \left(\frac{g_V^t}{e_t} g_V^e \frac{M_V^2}{M_V^2 - m_Z^2 + i\Gamma_Z m_Z} - 1 \right),$$

$$a = \frac{g_V^t}{e_t} g_A^e \frac{M_V^2}{M_V^2 - m_Z^2 + i\Gamma_Z m_Z}$$

and

$$g_V^{e,t} = (2I_3^{e,t} - 4Q^{e,t} \sin^2 \theta_W)/2 \sin 2\theta_W,$$

$$g_A^{e,t} = -2I_3^{e,t}/2 \sin 2\theta_W.$$

The factor in front is due to the neutral-current enhancement of toponium production. (Note that the definition of Γ_0 does not include neutral-current effects.) Radiative corrections, which reduce the peak cross-section by a factor of ~ 0.6, are taken into account. As parametrization of the energy spread,

$$\delta W = \frac{0.767 \cdot 10^{-5} W[\text{GeV}]^2}{[3 - 0.122 \cdot 10^{-5} W[\text{GeV}]^3]^{1/2}}$$

was assumed[4]. In Fig. 1 the cross-section on top of the resonance is shown [normalized to $\sigma(e^+e^- \underset{\gamma}{\to} \mu^+\mu^-)$], and for comparison the total cross-section for e^+e^- annihilation (without top and QCD corrections). For a toponium of 80 GeV and including radiative corrections, the ratio between signal and background is around 1 : 2, and scanning for such resonances would be tedious. However, at the time when e^+e^- experiments will be able to study topo-

[4] J. M. Jowett: Private Communication.

nium, its rough location will be known from collider experiments. Together with the rather distinct signature of its decay modes, the enhancement should be sufficient to find and to study toponium.

Apart from single quark decays, which will be discussed later, all 1^3S_1 decays proceed through $t\text{-}\bar{t}$ annihilation. Since these rates are proportional to the wave function at the

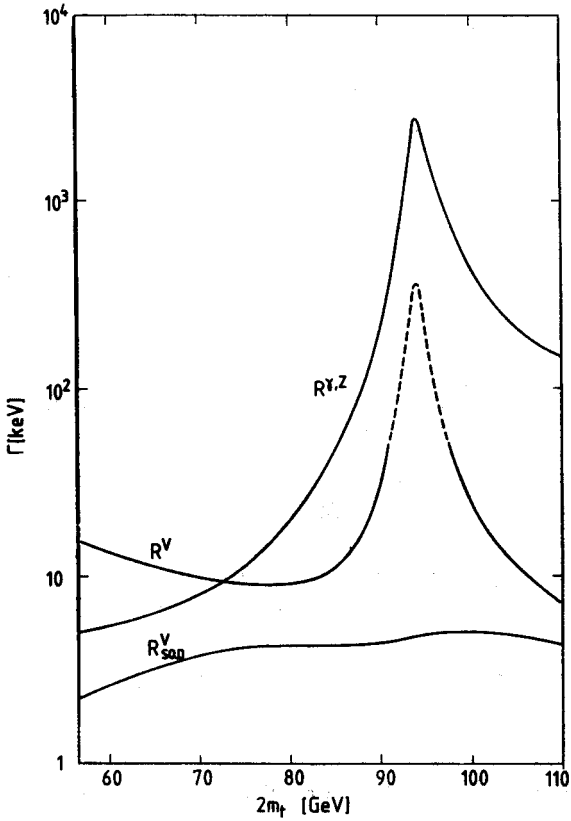

Fig. 1. Production cross-section for final states from hadronic and single quark decays of toponium on top of the resonance, relative to $\sigma(e^+e^- \xrightarrow{\gamma} \mu^+\mu^-)$, as a function of $M_{t\bar{t}}$ with the parameters described in the text. For comparison we show also the continuum cross-section. The dotted part of the toponium curve indicates the mass range where interference between resonance and continuum becomes important. In this range the curve is meant to indicate only the magnitude of cross-section changes. For a more detailed discussion see Ref. [25]. (From W. Buchmüller and J. H. Kühn, Contribution to LEPC working group.)

origin, their relative strengths can be predicted unambiguously. Owing to the decrease of α_s with increasing toponium mass, hadronic decays into three-gluon jets will become relatively less important (Fig. 2). The total rate for "fermionic" decays which may proceed through virtual photons, Z^0, and through W exchange is also shown in Fig. 2 for comparison. Up to a mass approximately 20 GeV below the mass of the Z, the total rate for these processes is hardly affected by the neutral current. Despite this, neutral-current effects

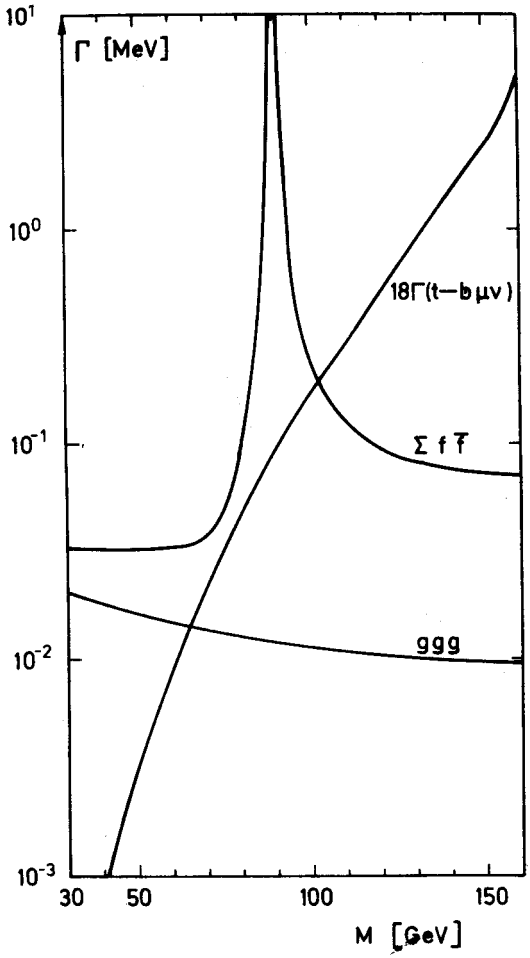

Fig. 2. Dominant decay modes of toponium (from Ref. [10])

will be observable and in some cases perhaps even be important for relatively light toponium owing to their interference with the dominant one-photon channel.

Off-resonance, also a parity-conserving quantity such as the forward/backward asymmetry contains an interference term linear in M_V^2/m_Z^2, whence these effects are even observed at PETRA or PEP. On-resonance, only the vector part of the neutral current couples to V. Thus only parity-violating terms are observable in leading order M_V^2/m_Z^2 and the polarization of a particle in the initial or final state has to be measured to be sensitive to an effect linear in A_{NC}/A_{em}. One quantity of interest is the difference in the toponium cross-sections for electrons with positive (R) or negative (L) helicities [12, 19] (see Fig. 3):

$$\delta \equiv \frac{\sigma_R - \sigma_L}{\sigma_R + \sigma_L} = \frac{2\,\mathrm{Re}\, va^*}{|v|^2 + |a|^2}\,, \tag{2.2}$$

where v and a have been defined in Eq. (2.1).

Note that this effect is maximal ($\delta = 1$) for M_V roughly 10 GeV below the mass of the Z. Its location is independent of quarkonium dynamics; however, it is extremely sensitive to the value of $\sin^2\theta_W$ and m_Z. This difference then leads to an alignment of the resonance spin S along the beam direction even for unpolarized beams:

$$\langle \vec{S}\vec{P}_e/|\vec{P}_e|\rangle = \delta, \tag{2.3}$$

which can be measured in single quark decays, as discussed below. Another way to measure essentially the same quantity is through the study of $\tau \to \pi\nu$ decays from $e^+e^- \to V \to \tau^+\tau^-$

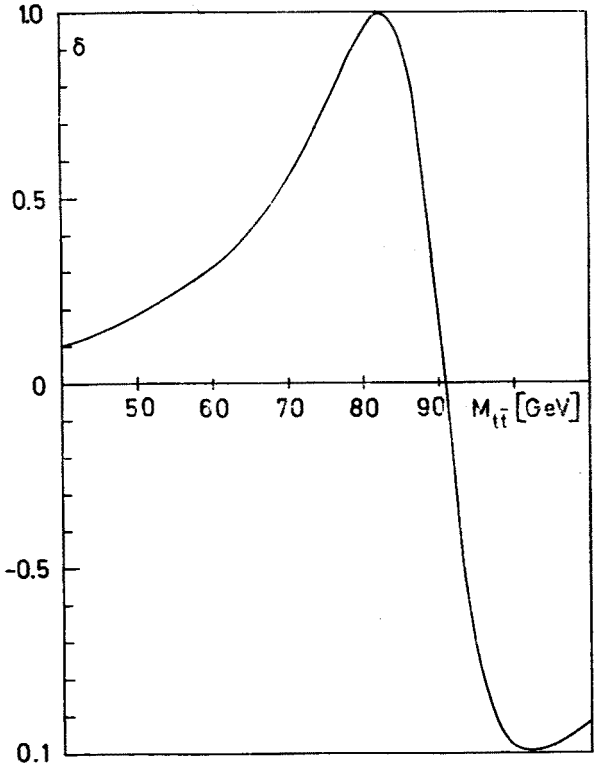

Fig. 3. Relative difference between toponium production cross-section for right-handed and left-handed beams $\delta = (\sigma_R - \sigma_L)/(\sigma_R + \sigma_L)$ as a function of M_V (from Ref. [13])

which are sensitive to the τ polarization. Unpolarized τ's would lead to a flat energy spectrum of π's (or ρ's). A linear term in dN/dx_π will be proportional to the τ helicity, which in turn is essentially determined by the coupling of toponium to the vector part of the neutral current. This has been discussed elsewhere in some detail (see Refs. [20] to [22]).

Of course, once the mass of toponium is sufficiently close to m_Z, terms of order $(A_{NC}/A_{em})^2$ become equally important. Then a sizeable forward-backward asymmetry of muons and of quark jets is expected, which is in general completely different from the asymmetry in the continuum region. This could lead to an accurate determination of the

neutral-current coupling of toponium. These issues, together with the special role of b-quark jets due to W exchange, are discussed in detail in Refs. [10] and [12].

The rate for SQD increases dramatically with increasing mass:

$$\Gamma_{\mathrm{SQD}} = 2 \cdot 9 \frac{G_F^2 m_t^5}{192\pi^3} f\left(\frac{m_t^2}{m_W^2}, \frac{m_b^2}{m_t^2}\right),$$

$$f(\varrho, \mu) = 2 \int_0^{(1-\sqrt{\mu})^2} du \frac{[(1-\mu)^2 + u(1+\mu) - 2u^2]}{(1-u\varrho)^2} [1+\mu^2+u^2-2(\mu u+\mu+u)]^{1/2}, \tag{2.4}$$

where f represents the corrections [9, 11] due to phase-space effects and the W propagator and is shown in Fig. 4. Already for $M_V \approx 65$ GeV it is as important as the three-gluon decay, and for sufficiently large top mass it dominates all other modes. Only in the narrow mass range $m_Z \pm \sim 10$ GeV does the dramatic enhancement of decays through the neutral current win against all competing channels. Since the rate for SQD is independent of the wave function it is the same for the ground state and for radial excitations.

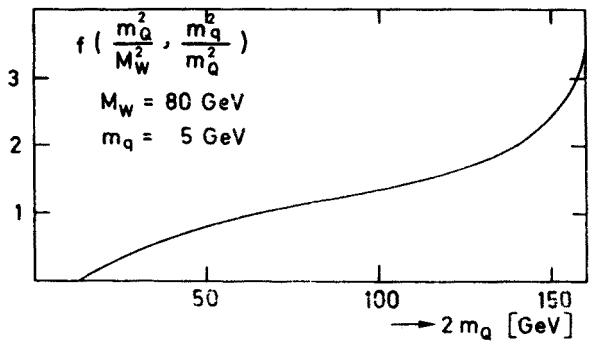

Fig. 4. Kinematic factor for single-quark decay [Eq. (2.4)] (from Ref. [10])

The production cross-section for events with SQDs in e^+e^- collisions,

$$\frac{\sigma_{\mathrm{top}} \cdot \mathrm{Br}\,(\mathrm{SQD})}{\sigma(e^+e^- \underset{\gamma}{\rightarrow} \mu^+\mu^-)} = \frac{9\pi}{2\alpha^2\sqrt{2\pi}} [|v|^2+|a|^2] \frac{\Gamma_0}{\sigma_W} \left[\left(\frac{2\delta W}{M_V}\right)^t + \varepsilon\right] \frac{\Gamma_{\mathrm{SQD}}}{\Gamma_{\mathrm{tot}}} \tag{2.5}$$

is nearly independent of the wave function [13] which cancels approximately in the ratio $\Gamma_{e^+e^-}/\Gamma_{\mathrm{tot}}$ for $M_V \lesssim 70$ GeV. Using a luminosity[5] of 10^{31} cm^{-2} s^{-1} one expects 150 (100) hadronic resonance events, and among these 60 (50) SQDs for a mass of 70 GeV (80 GeV) per day of running at LEP.

Compared with current-mediated decays into two-quark jets or hadronic decays into three-gluon jets the properties of SQDs will be rather striking: isolated leptons plus missing

[5] The nominal luminosity at 110 GeV is expected [23] to be 1.3×10^{31} cm^{-2} s^{-1}.

energy from semileptonic decays; nearly isotropic events with six jets from non-leptonic decays. As shown in Fig. 5, semileptonic and non-leptonic decays could be isolated for toponium masses as low as 50 GeV. On the other hand, even in the unfortunate case of near degeneracy of Z^0 and V, where the branching ratio decreases to $\sim 1\%$, they could still be separated from the $q\bar{q}$ decays owing to their striking signature.

The rate for SQD is a rather model-independent measure of the strength of charged-current couplings. Their appearance at the predicted level will prove that the new quark and b indeed belong in the same isodoublet. Furthermore, the angular distribution of

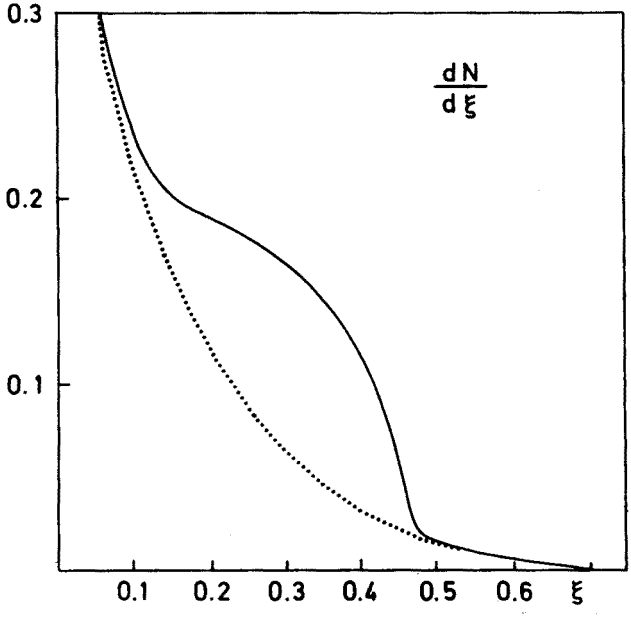

Fig. 5. Lepton spectrum from SQD plus background from semileptonic bottom and charm decay ($m_t = 25$ GeV). Dotted line: solely background (from Ref. [13])

leptons from SQDs can serve as an extremely useful tool for measuring the longitudinal polarization of toponium which is induced through $Z^0-\gamma$ interference [Eq. (2.2)]. The spins of t and $\bar{t}$ quarks are aligned with the spin of the $^3S_1$ bound state, and the degree of their polarization is also given by Eq. (2.2). The angular distribution of the leptons in the decay of fully polarized t quarks at rest,

$$\frac{dN}{d\cos\theta} \propto (1+\cos\theta), \tag{2.6}$$

where

$$\theta = \sphericalangle(\vec{P}_l, \vec{S})$$

is, furthermore, independent of the lepton energy, so all asymmetries are unaffected by cuts in the lepton energy. Thus leptons from the mode

$$(t\bar{t}) \to T+\bar{B}+l+X \tag{2.7}$$

lead to a forward-backward asymmetry

$$A_1 = \frac{\int_0^1 d\cos\theta \frac{dN}{d\cos\theta} - \int_{-1}^0 d\cos\theta \frac{dN}{d\cos\theta}}{\int_{-1}^1 d\cos\theta \frac{dN}{d\cos\theta}} = \tfrac{1}{2}\delta. \tag{2.8}$$

Leptons from the mode

$$(t\bar{t}) \to \begin{matrix} \bar{T}+X \\ \lfloor\!\to l+X \end{matrix}$$

constitute 50% of our "prompt" lepton signal. In this case 50% of the original quark polarization is retained through the hadronization, i.e. the formation of T and T* mesons and their subsequent weak decay [13]. For the overall asymmetry we therefore expect

$$A = \tfrac{3}{8}\delta, \tag{2.9}$$

where δ denotes the longitudinal V polarization calculated in Eq. (2.2). For a mass of 70 GeV (80 GeV) this amounts to 21% (35%). Considering the branching ratio into prompt leptons of nearly 7%, one may indeed hope to test these ideas.

A rather peculiar situation would occur if $|m_Z - M_V| \lesssim 5$ GeV. As already mentioned above, decays through a virtual Z^0 would dominate, and the total rate could reach up to $\sim$ 20 MeV in the extreme case. Branching ratios, final-state topologies, forward-backward asymmetries, and all other properties of the final state would be dominated by decays through the Z^0. (An alternative way of describing this scenario is through the V–Z mixing formalism [24, 25].) Even in this extreme case the energy spread δW will be substantially larger than the total width. Nevertheless, interesting interference effects could be observed in this case, which could even turn the resonance enhancement into a dip. More details can be found in Ref. [25].

2.2. Toponium P-states and radial excitations of V[6]

In contrast with the previous discussion of the ground state, various properties of P-states and of radial excitation are more sensitive to the details of the potential. In the following we will compare the predictions based on two QCD-inspired potentials, V_R [26] and V_T [15], defined through

$$\tilde{V}_R(\vec{q}^2) = -\tfrac{4}{3}\frac{12\pi}{27}\frac{1}{\vec{q}^2}\frac{1}{\ln(1+(\vec{q}/398\ \text{MeV})^2)}, \tag{2.10}$$

$$V_T(r) = -\frac{16\pi}{25}\frac{1}{rf(r)}\left[1+\frac{2\gamma_E+53/75}{f(r)}-\frac{462\ln f(r)}{625 f(r)}\right]+a\sqrt{r}+c, \tag{2.11}$$

[6] This section is largely based on Ref. [15].

where

$$f(r) \equiv \ln (1/(\Lambda_{\overline{\mathrm{MS}}} r)^2 + b)$$

and

$$a = 0.63\ \mathrm{GeV}^{3/2}, \quad b = 20, \quad c = -1.39\ \mathrm{GeV}, \quad \Lambda_{\overline{\mathrm{MS}}} = 140\ \mathrm{MeV}.$$

The numerical results for level spacings, $R(0)$ and $R'(0)$, and dipole matrix elements of the lowest levels and for various masses are given in Ref. [15].

Apart from the level spacings between the low-lying resonances, also $R^2(0)$ and $R'(0)^2$ differ up to a factor of 2 for the lowest levels. However, the qualitative features of P-states are common to all models and can be understood relatively easily:

Light quarkonium P-states are typically relatively broad objects with widths of several MeV for charmonium. Their annihilation amplitudes are proportional to the first derivative of the wave function at the origin $R'(0)$ and thus proportional to v/c. For increasing quarkonium mass, one thus expects strongly decreasing hadronic widths — quite in contrast with the behaviour of S-waves with roughly constant (up to a factor of 1 to 3) two- and three-gluon rates.

Similarly the rates for the dipole transition $\mathrm{P} \to \mathrm{S} \to \gamma$ will decrease. There is little variation from the factor k^3 which appears in the rate formula, since typical mass differences do not vary rapidly with the mass. However, the rates are also proportional to the dipole matrix element which, like typical bound-state radii, decreases strongly with mass. These statements can be made more quantitative as follows: the hadronic widths of triplet P-states are given by

$$\Gamma(2^{++} \to \mathrm{gg}) = \tfrac{128}{5} \alpha_s^2 \frac{R'(0)^2}{M_P^4}$$

$$\Gamma(0^{++} \to \mathrm{gg}) : \Gamma(1^{++} \to \mathrm{gq\bar{q}}) : \Gamma(2^{++} \to \mathrm{gg})$$

$$= \tfrac{15}{4} : \tfrac{25}{9} \frac{\alpha_s}{\pi} \ln \frac{M_P}{0.6\ \mathrm{GeV}} : 1. \tag{2.12}$$

For potentials $V(r) = \lambda r^\nu$, scaling laws [3] have been derived for quantities with the dimension of lengths L and for level spacings ΔM:

$$L \sim M^{-1/(2+\nu)}; \quad \Delta M \sim M^{-\nu/(2+\nu)}. \tag{2.13}$$

Up to variations of α_s^2 one then finds

$$\Gamma(0^{++} \to \mathrm{gg}) \sim L^{-5} M^{-4} \sim M^{-(3+4\nu)/(2+\nu)} \sim M^{-3/2} \Delta M^{5/2}, \tag{2.14}$$

where the last form has been adopted to facilitate comparison with potential model results. The scaling laws for dipole transitions have already been derived [3]:

$$\Gamma(\mathrm{P} \to \mathrm{S} + \gamma) \sim M^{-(2+3\nu)/(2+\nu)} \sim M^{-1} \Delta M^2. \tag{2.15}$$

For all phenomenologically interesting potentials the effective exponent ν in the region between 0.1 and 1 fm is close to zero and we thus expect that annihilation and dipole

rates of toponium P-states will be far smaller than those of charmonium. Their relative importance varies less drastically; nevertheless dipole transitions will dominate for sufficiently large masses,

$$\frac{\Gamma(0^{++} \to gg)}{\Gamma(P \to S+\gamma)} \sim M^{-(1+\nu)/(2+\nu)} \sim (\Delta M/M)^{1/2} \tag{2.16}$$

and this trend is even more pronounced owing to the decrease of α_s. As we shall see later, specific potential models will indeed lead to branching ratios for radiative transitions around 80% for toponium P-states with bound-state masses up to 70 GeV.

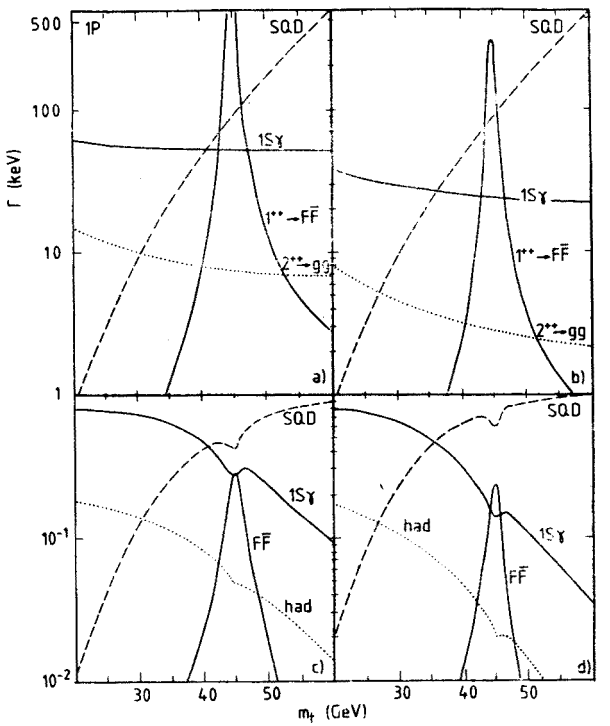

Fig. 6a, b) Partial widths for decay modes of the 1P-state as a function of the t-quark mass: $f\bar{f}$ stands for the sum of all fermion-antifermion pairs [a) Richardson potential; b) potential T]; c, d) Statistically weighted branching ratios $\sum_J (2J+1)/9\ \mathrm{Br}(P_J \to X)$ for the same decay modes [c) Richardson potential; d) potential T]

(from Ref. [15])

Owing to the narrowness of P-states the SQDs become important for S- and P-states at the same time, and dominate the dipole transitions for $M_V \gtrsim 70$–80 GeV. The resulting decay rates and branching ratios of 1P- and 2P-states are shown in Figs. 6 and 7. Up to this mass region there is also a chance to populate P-states through dipole transitions from 2S- or 3S-states. The rates and branching ratios, which are shown in Fig. 8 for V_T and in

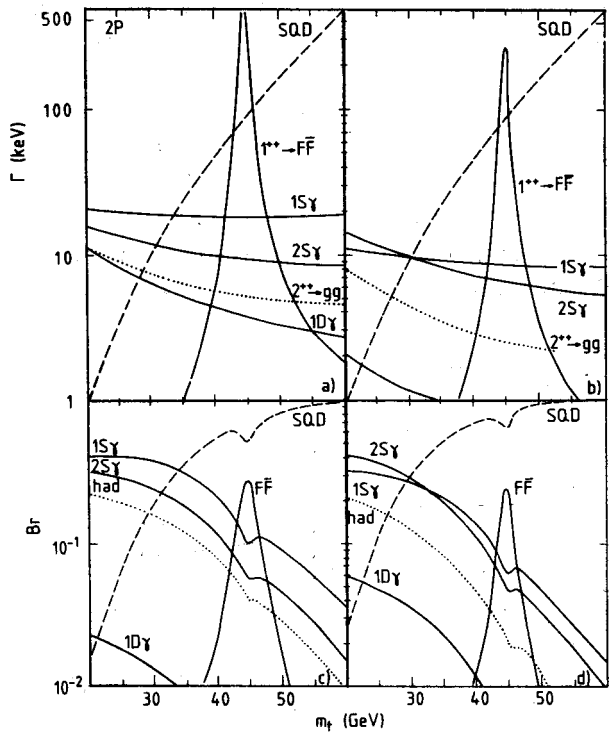

Fig. 7. Same as Fig. 6 for 2P-states (from Ref. [15])

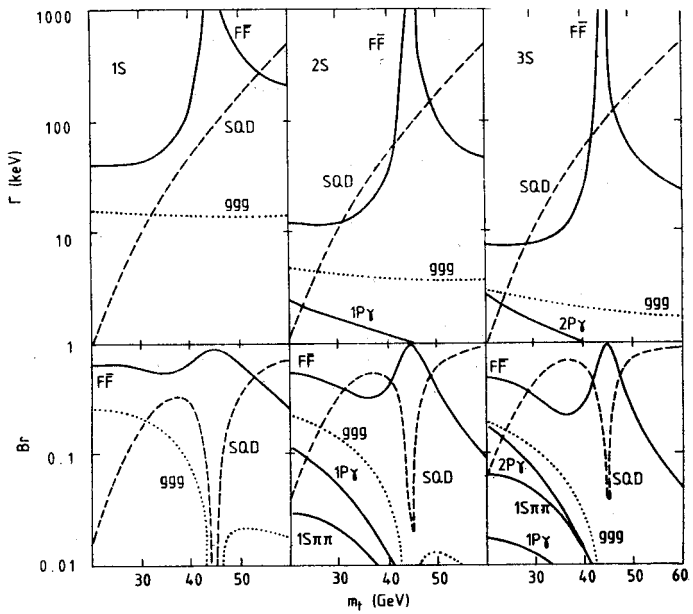

Fig. 8. Dominant decay modes and branching ratios of 1S-, 2S- and 3S-states, as calculated for the Richardson potential (from Ref. [15])

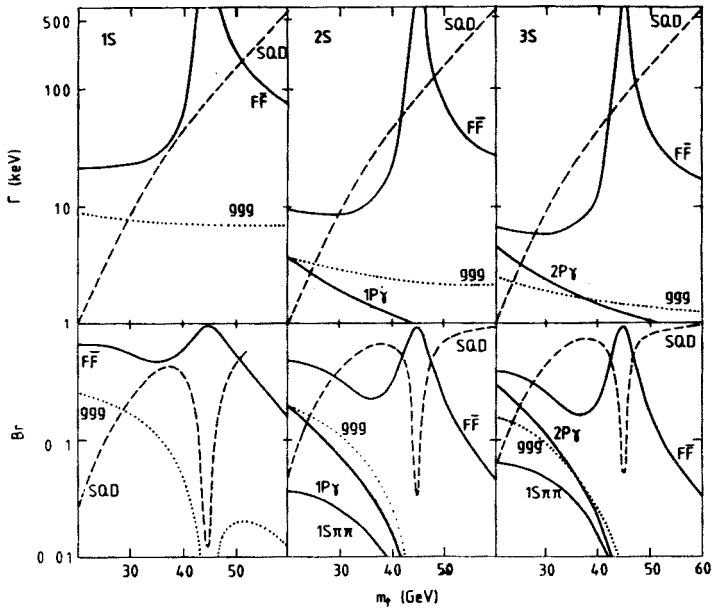

Fig. 9. Same as Fig. 8 for potential T (from Ref. [15])

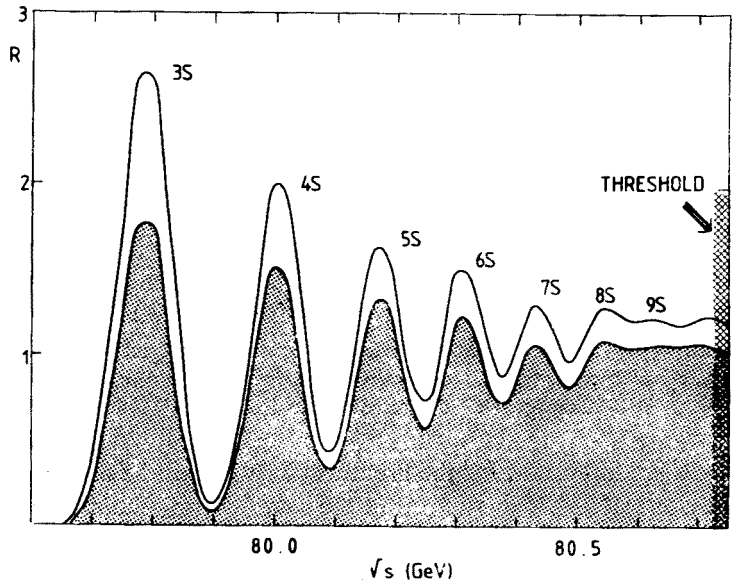

Fig. 10. Production cross-section for high radial excitations: $m_t = 40$ GeV, $\delta W = 40$ MeV. Shaded area: fraction of single-quark decays. For a more detailed discussion, see Ref. [25b]

Fig. 9 for V_R, are to some extent model-dependent. In any case, they decrease drastically with increasing mass. For $M_V = 50$ GeV, one still expects $\sum_J \mathrm{Br}(2^3S_1 \to \gamma + {}^3P_J) \approx 6$–$12\%$. However, already for 80 GeV this value decreases to 1–2%. (To resolve the fine-structure splitting of P-states will be even more difficult; $M(^3P_2) - M(^3P_0)$ has been estimated [5] to be around 10 MeV for the mass region of interest.)

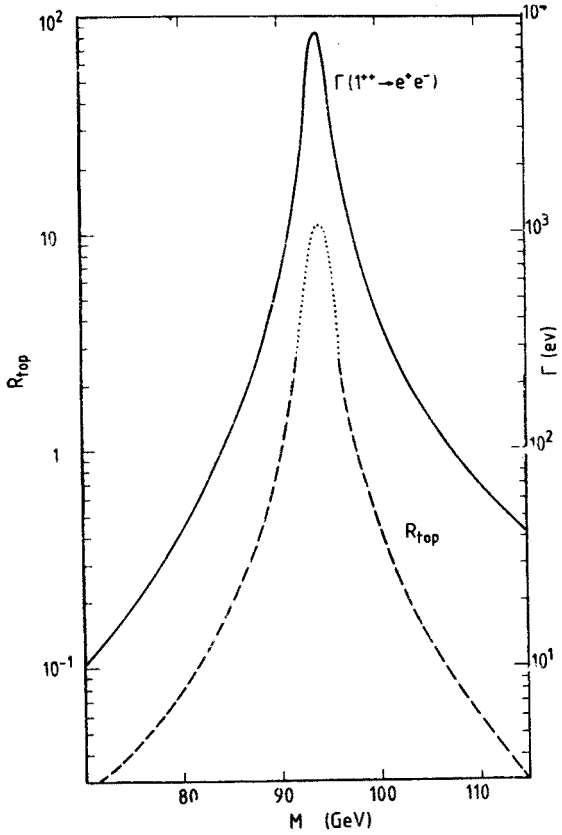

Fig. 11. Production of $1\ ^3P_1$ through the neutral current. Solid line: partial width into e^+e^-; dashed line: production cross-section on top of the resonance normalized to $\sigma(e^+e^- \xrightarrow{\gamma} \mu^+\mu^-)$. The dotted part of the toponium curve indicates the mass range where interference between resonance and continuum becomes important. In this range the curve is meant to indicate only the magnitude of cross-section changes. For a more detailed discussion see Ref. [25a]

Once the SQDs are important for the ground state they will be even more important for the excited levels; Γ(SQD) is constant, but the rate for annihilation decays is smaller for radial excitations. Also the rates for dipole transitions are smaller. In addition, P-states decay dominantly via SQD or cascade to a lower-lying S-state, and there the story repeats itself. Thus higher excitations could be quite efficient top factories even below the nominal $T\bar{T}$ threshold, and for masses above 70 GeV it could become difficult to establish this thresh-

old experimentally. Figure 10 illustrates this situation for a mass value of 80 GeV suggested by recent collider results. We show the contribution to R from the radial excitations $V^{(4)}-V^{(10)}$, where we take an energy spread of 40 MeV into account but ignore radiative corrections and neutral-current effects. The shaded area indicates the fraction of events which contribute to SQDs. The dashed curve represents the result for massless quarks

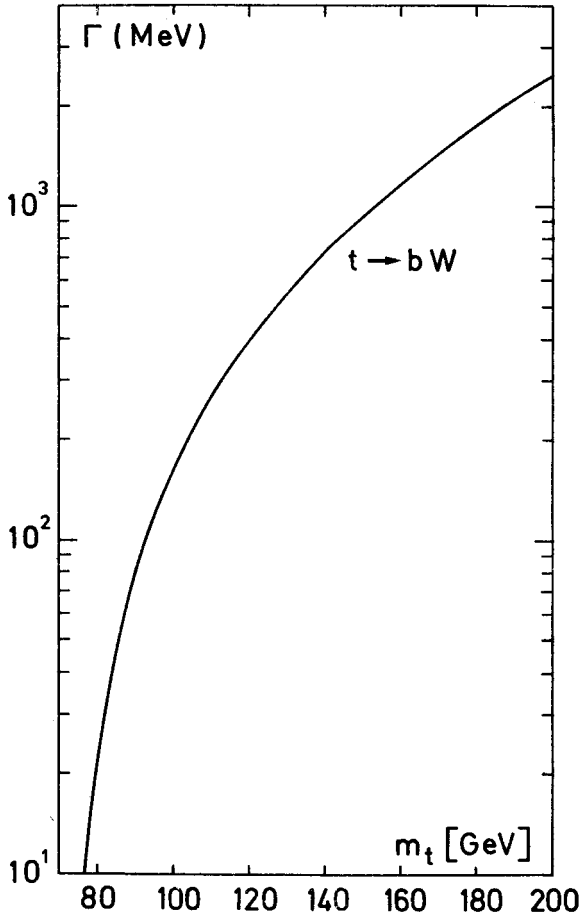

Fig. 12. Rate for the semiweak decay $t \to bW$

(neglecting mass and QCD corrections), i.e. 4/3, which is approximately dual to the sum of resonances. Toponium production above the 4S will thus look almost like top production above the $T\bar{T}$ threshold[7].

The question has been raised whether $^3P_1$ states could be produced directly through the axial part of the neutral current, since weak and electromagnetic couplings are of comparable strength and the former are even enhanced through the Z^0 propagator [27].

[7] A more detailed discussion of this effect will be published elsewhere [25b].

However, production of P-states is determined by the derivative of the wave function at the origin:

$$\Gamma(^3P_1 \to e^+e^-) = \frac{(1-4\sin^2\theta_W)}{4\pi^2} G_F^2 \frac{|R'(0)|^2 m_Z^4}{(M^2-m_Z^2)^2-\Gamma_Z^2 m_Z^2}. \tag{2.17}$$

R'^2 is proportional to v^2/c^2 and is strongly suppressed for heavy quarkonia. Quantitative estimates show that the optimal signal-to-background ratio of $\sim 0.5\%$ (corresponding

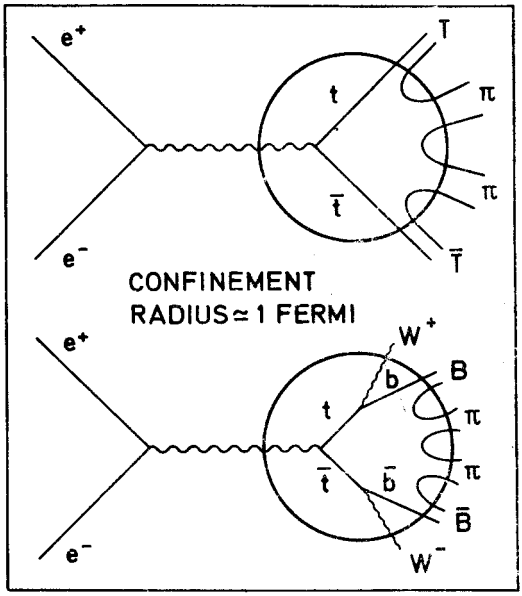

Fig. 13. Space-time picture of top production in e^+e^- annihilation. a) The weak decay rate of t is far less than 2 fm^{-1}. The T mesons are produced and decay far away from the production point. b) The weak decay rate of t is far larger than 2 fm^{-1}. The t-quark decays within the confinement region. No T mesons are produced

to R_{top} of ~ 0.1) will be reached between 70 and 80 GeV. To illustrate this result, we show in Fig. 11 $\Gamma(^3P_1 \to e^+e^-)$ and R on top of the resonance, which should be compared with the continuum contribution shown in Fig. 1. A P-state with this mass would either decay weakly through SQD or would decay into $1S+\gamma$. The 1S-state in turn has a sizeable branching ratio for SQDs. It is thus perhaps not excluded that direct resonant formation of P-states could be observed in this manner.

2.3. Superheavy quarks [9, 10, 16]

If m_t should be far larger than expected, or if a fourth generation of quarks exists, the semiweak decay into a real W and its lighter isodoublet partner may be kinematically allowed. Even if suppressed by weak mixing angles as expected for the next b-type quark, this reaction could still compete with annihilation decays, and their relative strength could

eventually be used to determine these angles. For the Cabibbo-allowed decays $\hat{t} \to \hat{b}+W$ and for masses of $\hat{t}$ above 100 GeV, the width (Fig. 12)

$$2\Gamma(\hat{t} \to \hat{b}+W) = 2\frac{G_F}{8\pi\sqrt{2}} m_{\hat{t}}^3 \left(1+2\frac{M_W^2}{m_{\hat{t}}^2}\right)\left(1-\frac{M_W^2}{m_{\hat{t}}^2}\right)^2 \tag{2.18}$$

exceeds 200 MeV (≈ 1 fm^{-1}) and our notion of top mesons breaks down. The heavy quark decays, even before it has time (≈ 1 fm/c) to form a meson with spatial extension of ≈ 1 fm together with a light quark out of the sea (Fig. 13). As a clear signature for such a situation, one expects that the angular distributions of all decay products (W, leptons) follow the predictions of the free quark model. Remember that these distributions are quite different if the quarks first convert into scalar or vector mesons.

Similarly the whole concept of quarkonia breaks down for $m_t \gtrsim 200$ GeV. Then the decay width of its constituents of roughly 1 GeV is comparable to the mass difference between the ground state and the radial excitations. This corresponds to the situation where the t-quark lifetime is smaller than the characteristic time of revolution. We thus arrive finally at a situation where the t-quark decays before it can participate in strong interactions.

3. Supersymmetry and toponium decays

3.1. Gluino production through virtual gluons [28]

A number of toponium decays have been proposed which could allow some of the particles predicted by supersymmetry to be detected and their masses and couplings to be determined. The drastically different scenarios which are summarized in Tables I and II depend on the choice of the unknown masses of t and of the various postulated particles. In the following we will not try to be completely general and cover all possibilities, but rather we will discuss a few of the most promising choices.

Toponium (and Υ) decays as a mean of searching for gluinos have already been proposed some time ago [28]. Being electrically neutral, gluinos are hard to produce in e^+e^- collisions. However, as colour octets they may be pair-produced either in hadronic collisions or in toponium decays through the processes indicated in Fig. 14a, b. Evidently the rate for these processes depends on the gluino mass only and is independent of all other SUSY parameters — quite in contrast with the reactions to be discussed later. Compared with the production of heavy quarks (charm, bottom) the rates are enhanced by a factor $1/2 \sum f_{abc}^2 / \sum (\lambda_{ij}^a/2)^2 = 3$. In Fig. 15a we show the rates for $^3S_1$ and in Fig. 15b those for P-states as a function of $m_{\tilde{g}}$ normalized to their dominant conventional hadronic decay rate

$$R(^3S_1) \equiv \Gamma(gg\tilde{g}\tilde{g})/\Gamma(ggg), \tag{3.1a}$$

$$R(^3P_0, {}^3P_2) \equiv \Gamma(g\tilde{g}\tilde{g})/\Gamma(gg), \tag{3.1b}$$

$$R(^3P_1) = \Gamma(g\tilde{g}\tilde{g})/\Gamma(gq\bar{q}) \tag{3.1c}$$

for fixed $m_V = 80$ GeV and a binding energy of 1.5 GeV for the P-states ($\alpha_s \equiv 0.15$). (We used the analytic forms given in Ref. [28b] for heavy quark production.) For light gluinos these ratios can become quite sizeable: up to 20% for S-states and even up to 60%

TABLE I

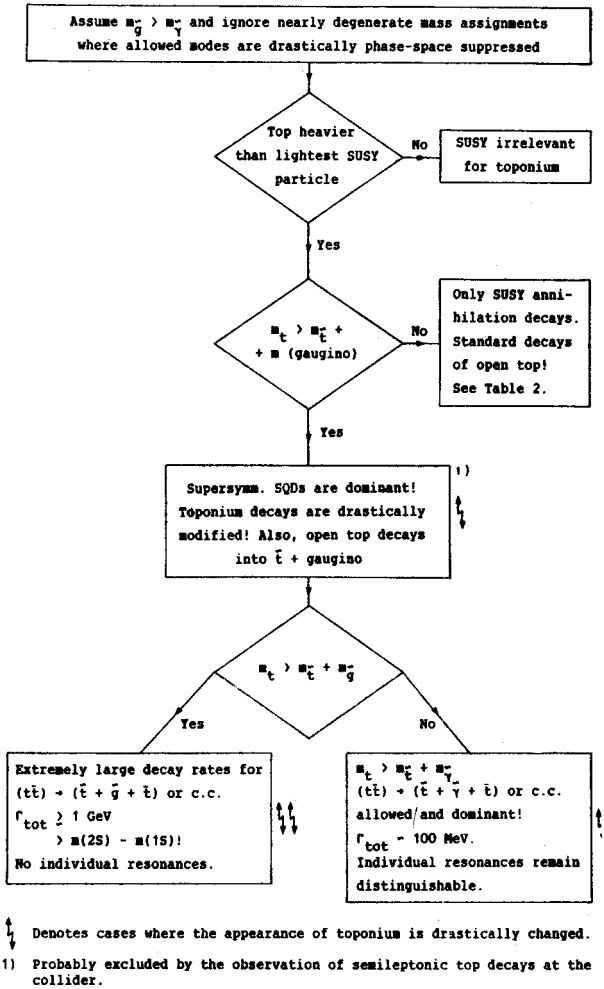

for P-states. However, as indicated in Figs. 6 to 9, the hadronic branching ratios themselves become relatively small for a heavy toponium. As a specific example, let us consider $M_V = 80$ GeV. To obtain the overall branching ratio, the ratio $R(^3S_1)$ has to be multiplied by ~ 0.1, the P-state ratios $R(^3P_J)$ by 0.20, 0.03, and 0.07 for $J = 0, 1, 2$. Furthermore, taking the branching ratio for dipole transitions into account, one finds at best

TABLE II

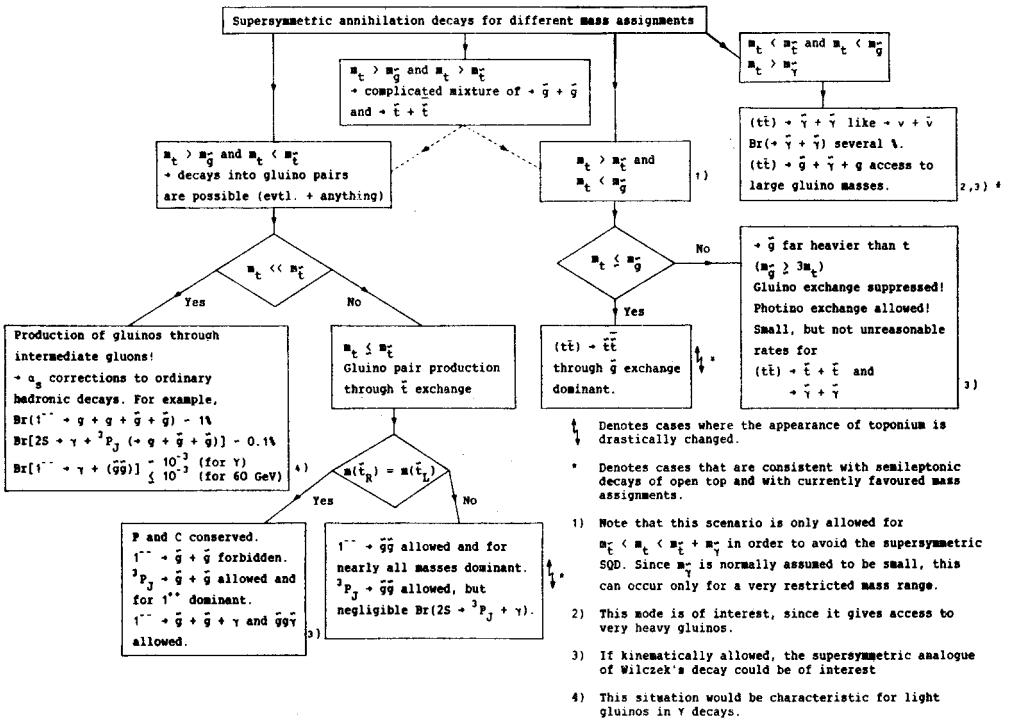

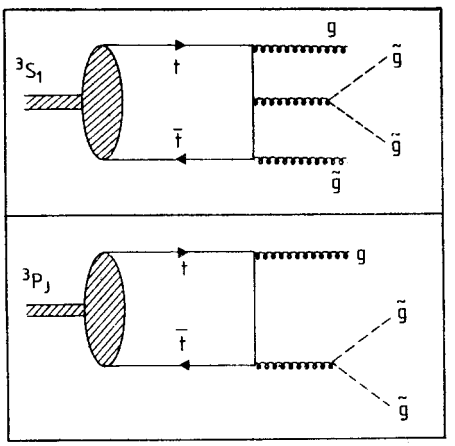

Fig. 14. Lowest-order diagrams for gluino production in toponium decays through virtual gluons

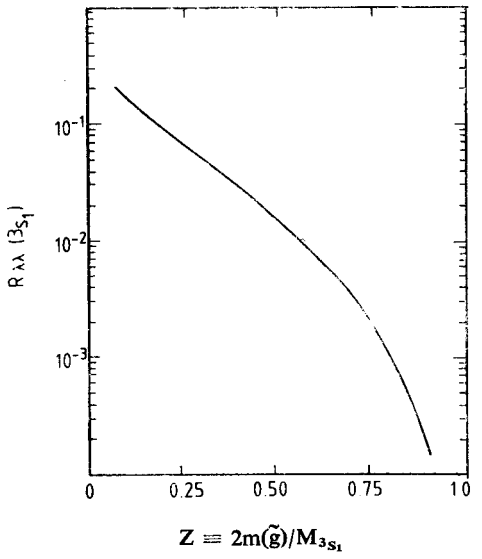

a

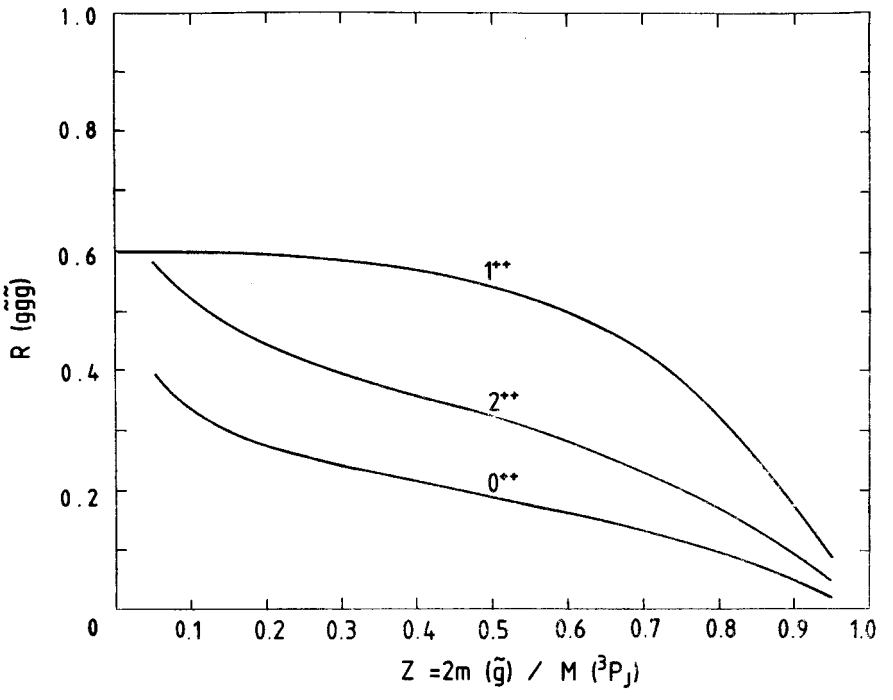

b

Fig. 15. Decay rate for toponium into gluinos and gluons, relative to their dominant conventional hadronic decay rate as defined in Eq. (3.1): a) $^3S_1$ decays (from Ref. [28]); b) ^3P_J decays

($m_{\tilde{g}} = 5$ GeV)

$$\mathrm{Br}\,(1S \to gg\tilde{g}\tilde{g}) \approx 10^{-2},$$

$$\sum_J \mathrm{Br}\,(2S \to \gamma + {}^3P_J(\to g\tilde{g}\tilde{g})) \approx 10^{-3}.$$

The rates are higher by a factor of ~ 3 for ${}^3S_1$ and by a factor of ~ 10 for P-states, if $M_V = 70$ GeV, but the experimental verification still looks quite difficult. For heavier gluinos these branching ratios rapidly become worse[8].

3.2. Gluino production through virtual squark exchange ($m_{\tilde{g}} > m_t$)

A number of authors [31, 32] have speculated that the scalar partner of top could be the lightest of all squarks with a mass comparable to m_t. This would lead to sizeable branching ratios for toponium decays into gluino pairs through squark exchange (Fig. 16). The rate would be proportional to α_s^2 and thus could even dominate in some cases. Since this mode also leads to a rather clean signature (two-body decay into energetic gluinos!) it is quite a promising candidate for gluino searches.

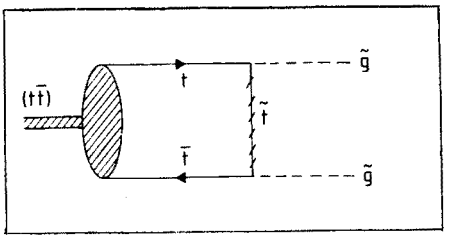

Fig. 16. Feynman diagram for gluino pair production in toponium decays through s-top exchange

To understand the relevance of this channel for the various ($t\bar{t}$) states, we first discuss the selection rules for decays into two Majorana fermions.

The quantum numbers of a fermion-antifermion system are given by

$$P = -(-)^L; \quad C = (-)^{L+S}. \tag{3.2}$$

This result holds true also for Majorana particles. From the requirement of antisymmetric wave functions for identical fermions, one derives in addition

$$L = \begin{Bmatrix}\text{even}\\ \text{odd}\end{Bmatrix} \Leftrightarrow S = \begin{Bmatrix}0\\ 1\end{Bmatrix}. \tag{3.3}$$

This implies that two Majorana particles can only have the following quantum numbers: 0^{-+}; 0^{++}, 1^{++}, 2^{++}; 2^{-+}; ...;. Hence, if parity or charge conjugation are conserved, ${}^3S_1(1^{--})$

[8] Recent collider results presumably exclude gluino masses in the range ~ 10 to 40 GeV [29]. For light gluinos the situation remains controversial [29, 30]. In any case, if $m_{\tilde{g}}$ is below 4 GeV, Υ decays are more promising: either through a detailed study of ${}^3P_1$ ($b\bar{b}$) or through a search for gluino-gluino bound states in radiative Υ decays (see Section 4).

$\to \tilde{g}\tilde{g}$ is forbidden, and $^1S_0(0^{-+}) \to \tilde{g}\tilde{g}$ and $^3P_J(J^{++}) \to \tilde{g}\tilde{g}$ are allowed. In general, however, the scalar partners of right- and left-handed quarks are expected to have different masses; parity and charge conjugation symmetry are violated; and $^3S_1 \to \tilde{g}\tilde{g}$ is allowed [31–33] and is usually even dominant. For completeness we list all relevant decay rates:

$$\Gamma(0^{-+} \to \tilde{g}\tilde{g}) = \tfrac{2}{3}\, 2^6 \alpha_s^2 \left(\frac{R(0)}{M}\right)^2 a_5^2 \left(\frac{m_{\tilde{g}}}{M}\right)^2 \beta,$$

$$\Gamma(1^{--} \to \tilde{g}\tilde{g}) = \tfrac{2}{3}\,\tfrac{2^6}{3}\, \alpha_s^2 \left(\frac{R(0)}{M}\right)^2 a_1^2 \beta^3,$$

$$\Gamma(1^{+-} \to \tilde{g}\tilde{g}) = 0, \tag{3.4}$$

$$\Gamma(J^{++} \to \tilde{g}\tilde{g}) = \tfrac{2}{3}\, 2^{10} \alpha_s^2 \left(\frac{R'(0)}{M^2}\right)^2 \begin{cases} b_1^2 \left(\frac{m_{\tilde{g}}}{M}\right)^2 \beta^3 & J = 0, \\ (a_5 - b_1)^2 \beta & J = 1, \\ b_1^2\, \frac{1}{5} \left(\frac{3}{4} + \frac{2m_{\tilde{g}}^2}{M^2}\right) \beta^3 & J = 2, \end{cases}$$

where

$$\beta \equiv (1 - 4m_{\tilde{g}}^2/M^2)^{\frac{1}{2}},$$

$$a_{1,5} \equiv \tfrac{1}{2} \left(\frac{m_t^2}{-m_t^2 - m_R^2 + m_{\tilde{g}}^2} \mp \frac{m_t^2}{-m_t^2 - m_L^2 + m_{\tilde{g}}^2} \right),$$

$$b_{1,5} \equiv \tfrac{1}{2} \left(\frac{m_t^4}{(-m_t^2 - m_R^2 + m_{\tilde{g}}^2)^2} \pm \frac{m_t^4}{(-m_t^2 - m_L^2 + m_{\tilde{g}}^2)^2} \right).$$

In the extreme case where $m_L \approx m_{t'}$, $m_R \gg m_{L'}$, and $\beta \approx 1$, this mode would dominate all $^3S_1$ decays up to $M_V \approx 110$ GeV (excluding the tiny region $m_Z \pm 5$ GeV), but also for less extreme choices it would still be the dominant channel. Since this holds true also for radial excitations, decays into P-states would be quite suppressed. P-states could, however, play an important role, if parity and charge conjugation were conserved ($m_L = m_R$). In this case, dipole transitions from n^3S_1 to $\gamma + {}^3P_J$ would proceed with normal strength and P-states could subsequently decay into gluino pairs [33]. In Fig. 17 we therefore compare the corresponding rates for decays of 1^{++} and 2^{++} states with their conventional modes. If not suppressed by phase space, $^3P_1$ annihilation into $\tilde{g}\tilde{g}$ would even dominate the $^3P_1 \to {}^3S_1 + \gamma$ dipole transition, and one of the three photon cascades would be absent in this peculiar scenario.

It should be noted that instead of gluinos, also two photinos could be produced, and all previous formulae apply after the substitution $\alpha_s^2 \to 9/2\alpha^2 e_t^4$. The branching ratio is comparable to the one for e^+e^- decays and is thus non-negligible if gluino decays are kinematically forbidden. Since the decay products are invisible, this would effectively only reduce the visible cross-section by at most 10% and thus this decay mode would remain

unnoticed. Tagging the invisible channel through $2^3S_1 \to \pi\pi + 1^3S_1$ or $2^3S_1 \to \gamma\gamma + 1^3S_1$ is possible in principle; in practice, however, the combined branching ratios are rather low ($< 10^{-3}$).

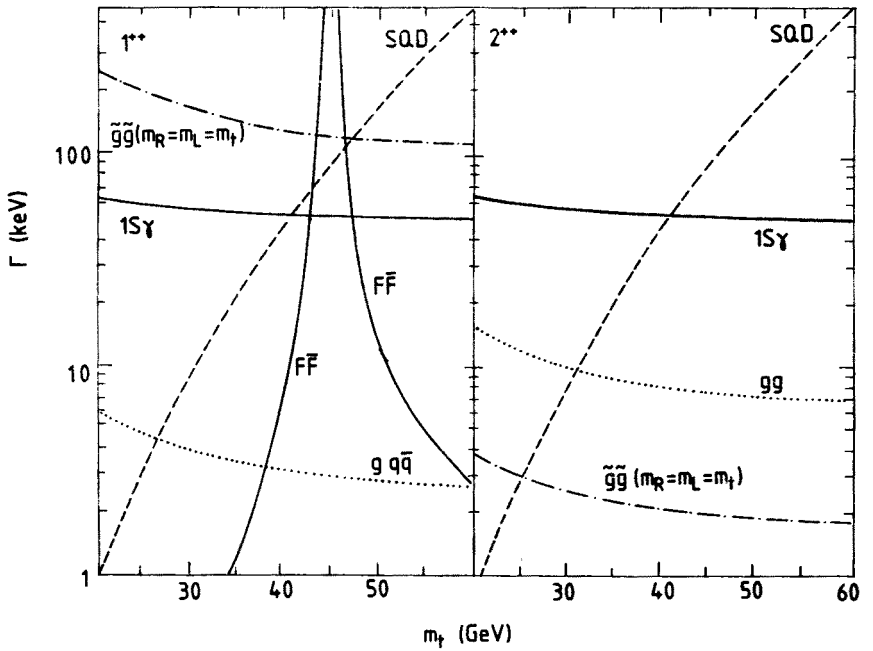

Fig. 17. Conventional decay rates of 1^{++} and 2^{++}, compared with their decay rate into two gluinos through squark exchange (from Ref. [33])

For completeness we should also mention that toponium decays into $\tilde{W}^0 + \tilde{\gamma}$ [32] and into $\tilde{\gamma}\tilde{g}g$ or $\tilde{\gamma}\tilde{g}\tilde{g}$ [34], as well as the supersymmetric analogue [32] of Wilczek's mechanism $^3S_1 \to \tilde{\gamma} + \tilde{H}$, have been considered in the literature.

3.3. Supersymmetric single-quark decays [$m_{\tilde{t}} + m_{\tilde{g}}$ (or $m_{\tilde{\gamma}}$) $< m_t$]

The mass assignment $m_{\tilde{t}} < m_t$ has been favoured by a number of currently discussed models. In this case toponium could drastically alter its appearance or even cease to exist as well-defined resonance. Although these scenarios are already ruled out if the semileptonic top decays observed by the UA1 Collaboration [2] are taken at face value, we nevertheless mention them for completeness.

Single-quark decays into a squark and a light gaugino (Fig. 18) — if kinematically allowed — can have an extremely high rate [31]:

$$\Gamma((t\bar{t}) \to \tilde{t} + \tilde{g} + \bar{t}) + \text{c.c.} = 2 \cdot \tfrac{2}{3}\, \alpha_s m_t \left(\frac{2\vec{P}_{\tilde{g}}}{m_t}\right)^2. \tag{3.5}$$

If not severely suppressed by phase space, the resulting width exceeds 1 GeV and is thus larger than the toponium level spacing. Obviously no $t\bar{t}$ resonances exist in this case.

This situation can be described in the following (semiclassical) space-time picture: the constituents' characteristic time of revolution would be large compared with their life time, and the notion of a bound state becomes meaningless.

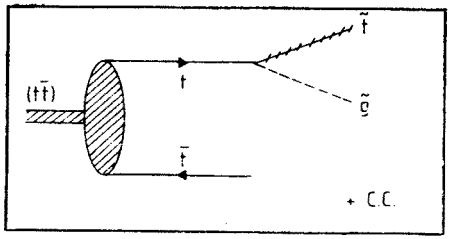

Fig. 18. Diagram for the decay of a quark in toponium into a squark plus gluino

Even if this hadronic mode is kinematically forbidden, the corresponding electromagnetic decay mode into a squark and a photino could still proceed at an appreciable rate:

$$\Gamma((t\bar{t}) \to \tilde{t} + \tilde{\gamma} + \bar{t}) + \text{c.c.} = 2 \cdot \tfrac{1}{2}\, \alpha Q_t^2 m_t \left(\frac{2\vec{P}_{\tilde{\gamma}}}{m_t}\right)^2. \tag{3.6}$$

Although not strong enough to wipe out toponium resonances, it would still dominate all other channels. However, it must again be stressed that if semileptonic top decays are observed at the collider, this scenario is no longer tenable.

An amusing borderline case would be the mass assignment $m_{\tilde{t}} + m_{\tilde{\gamma}} > m_t > m_{\tilde{t}}$. In this case $(t\bar{t}) \to \tilde{t} + \bar{\tilde{t}}$ mediated by gluino exchange could play the dominant role [31].

3.4. Goldstone fermions from non-linear realizations of supersymmetry

Recently a supersymmetric model has been proposed by Wess et al. [35], which differs drastically from those discussed until now. In their model, supersymmetry is realized in a non-linear form, and its only remnants at low energy are Goldstone fermions coupled to ordinary matter through the canonical energy momentum tensor. The additional term in the Lagrangian reads (see, for example, Ref. [36])

$$\mathcal{L}_\lambda = \frac{i}{4}\{\bar{\lambda}\gamma^\mu \partial_\mu \lambda - (\partial_\mu \bar{\lambda})\gamma^\mu \lambda\} - \tfrac{1}{2}\, m_\lambda \bar{\lambda}\lambda + i\kappa \bar{\lambda}\gamma^\mu \partial^\nu \lambda T_{\nu\mu}. \tag{3.7}$$

Here λ denotes the Goldstone fermion, T the canonical energy momentum tensor, and κ a constant of dimension M^{-4}. The mass term has been introduced by hand.

If the characteristic scale of κ is comparable to the mass of toponium, then decays into two Goldstone fermions could play an important role. Since these are weakly interacting particles, the missing-energy signature would be almost the same as the one of photino decays. There is, however, also a marked difference: since parity is conserved in the coupling of λ to ordinary matter, only states of positive charge conjugation could decay in this manner. The decay rates are extremely sensitive to the mass of toponium owing to the non-renormalizable interaction. Dimensional considerations lead us to expect branching

ratios proportional to $\kappa^2 M^8$. Decays of (pseudo) scalars are suppressed by $(m_\lambda/M)^2$ as a consequence of chiral invariance, just as in the photino and gluino case. The rates for 2^{++} decays have been given previously [36], and the complete list reads[9]:

$$\Gamma({}^3P_J \to \lambda\lambda) = \frac{3}{(2J+1)} \frac{3}{4\pi} \frac{R'^2}{M^4} \frac{\kappa^2 M^8}{4\pi} \left(1 - \frac{4m_\lambda^2}{M^2}\right)^{3/2} \begin{cases} \frac{4}{3} \frac{m_\lambda^2}{M^2} \\ 1 \\ 1 + \frac{8}{3} \frac{m_\lambda^2}{M^2} \end{cases} \quad \text{for} \quad \begin{cases} 0^{++} \\ 1^{++}, \\ 2^{++} \end{cases} \tag{3.8}$$

where R' denotes the derivative of the radial wave function at the origin and M the mass of the quarkonium system. The derivation of this formula is given in the Appendix.

It should be mentioned that the best limits obtainable from the $(b\bar{b})$ system are probably those resulting from a study of ${}^3P_1(1^{++})$ decays; ${}^3P_1$ is narrower than ${}^3P_2$ by roughly a factor of two, and its rate for $\lambda\lambda$ decay is larger by a factor of 5/3 (for $m_\lambda = 0$). The second advantage will persist for toponium (the total widths of P-states will be dominated by dipole transitions and will thus be approximately equal for all three of them). The absence of $2^3S_1 \to \gamma {}^3P_{1,2}$ $(\to {}^3S_1^{+\gamma})$ at the predicted level would then be a strong argument in favour of this model. Conversely, if the photon cascade is observed with the predicted strength, one derives the limit $\kappa^{-1/4} \gtrsim O(M_{t\bar{t}})$. [More specifically: for a 70 GeV $t\bar{t}$ system the limit $\mathrm{Br}(2S \to {}^3P_1\gamma \to {}^1S\gamma\gamma)_{\mathrm{exp}}/\mathrm{Br}(2S \to {}^3P_1\gamma \to 1S\gamma\gamma)_{\mathrm{theory}} > 0.5$ leads to $\kappa^{-1/4} \gtrsim 40$ GeV.]

Another possibility for finding Goldstone fermions and establishing limits on κ is the decay mode ${}^3S_1 \to \gamma + \lambda + \lambda$. Although it is of order $\alpha\kappa^2 M^8$, it is still quite useful since it leads to a rather clean signature: a single *hard* photon plus missing energy. The rate is given by [37]

$$\frac{\Gamma({}^3S_1 \to \gamma + \lambda + \lambda)}{\Gamma({}^3S_1 \underset{\gamma}{\to} e^+e^-)} = \frac{\kappa^2 M^8}{2^{10}\pi^3\alpha} K\left(\frac{2m_\lambda}{M}\right) \tag{3.9}$$

and the kinematic factor K can be also found in Ref. [37]. For $m_\lambda = 0$ this ratio amounts to 1.25×10^{-3} $(\kappa M^4)^2$. Again we realize that owing to the drastic M dependence, the bounds on $\kappa^{1/4}$ are not much improved through increased accuracy of measurements — it is essentially only M_V that counts.

Apparently the reaction with the maximal energy leads to the optimal limits on κ. A potentially interesting reaction is the decay $Z \to \lambda\lambda$ through intermediate quarks (Fig. 19). Strictly speaking, this reaction is outside the subject "quarkonium decays". Nevertheless, since it has not been discussed before in the literature, we shall briefly comment on this possibility. Although parity and charge conjugation of Z^0 are usually defined to be negative, this decay is possible through the axial coupling of the intermediate boson: $g_A^Q \bar{f}\gamma_\mu Z^\mu \gamma_5 f$. Quarks appear in isodoublets, $g_A^u + g_A^d = 0$; hence the rate would vanish if quarks within one doublet had equal masses. Therefore one expects the dominant contribution from the doublet with the largest splitting $\begin{pmatrix} t \\ b \end{pmatrix}$. The amplitude for $Z \to \lambda\lambda$ is con-

[9] The results for 0^{++} and 1^{++} have not been published elsewhere.

veniently written in the form

$$A(Z \to \lambda\lambda) = -ic_Z g_A \kappa M_Z^4 \bar{u}_\lambda E\!\!\!/ \gamma_5 v_\lambda, \tag{3.10}$$

where E denotes the polarization of Z, and $\bar{u}_\lambda$ and v_λ are spinors for the outgoing Goldstone fermions. The rate, normalized relative to the rate for decays into one species of neutrinos, is then given by

$$\frac{\Gamma(Z \to \lambda\lambda)}{\Gamma(Z \to \nu\bar{\nu})} = \tfrac{1}{4}\kappa^2 M_Z^8 |c_Z|^2 \left(1 - \frac{4m_\lambda^2}{M_Z^2}\right)^{3/2}. \tag{3.11}$$

The absorptive contribution to c_Z is finite. For a quark doublet with masses $m_t = m \neq 0$ and $m_b \approx 0$, one finds (see Appendix)

$$\operatorname{Im} c_Z = \frac{\pi}{(4\pi)^2}\left[-1+\theta(M_Z-2m)\left(1-\frac{4m^2}{M_Z^2}\right)^{3/2}\right]. \tag{3.12}$$

The individual contribution from each quark species to the dispersive (real) part is quadratically divergent. This leading divergence is cancelled within one doublet, and the remaining

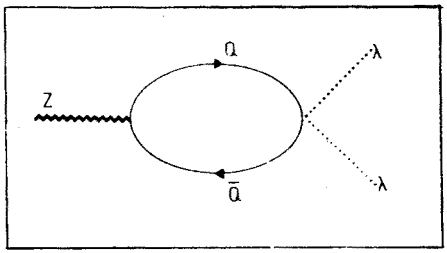

Fig. 19. Feynman diagram for Z decays into Goldstone fermions through virtual quarks

logarithmic divergence should be cut off at a scale $\Lambda = O(\kappa^{-1/4})$. The final result is not very sensitive to the precise value of Λ. In the Appendix we find

$$\operatorname{Re} c_Z = \frac{1}{(4\pi)^2}\left[-3\frac{m^2}{M_Z^2}\ln\frac{4\Lambda^2}{M_Z^2} - \tfrac{13}{2}\frac{m^2}{M^2} + 2\ln 2\right.$$

$$\left. - \left(1-6\frac{m^2}{M_Z^2}\right)\ln\frac{4m^2}{M_Z^2} - \left(1-\frac{4m^2}{M_Z^2}\right)\sqrt{\left|1-\frac{4m^2}{M^2}\right|}\ln\frac{1+\sqrt{\left|1-\frac{4m^2}{M_Z^2}\right|}}{1-\sqrt{\left|1-\frac{4m^2}{M_Z^2}\right|}}\right]. \tag{3.13}$$

All limits on the branching ratios of Z into invisible channels ("species of neutrinos") can be immediately translated into bounds on κ once m_t or lower limits on m_t are known.

For example, from the cut-off independent absorptive part alone, and for $2m_t \approx m_Z$, one derives

$$\kappa^{-1/4} > 0.24\, M_Z n^{-1/8}, \tag{3.14}$$

where n denotes the limit on invisible Z decay modes in units of neutrino species. Including the dispersive part with a value of Λ of order m_Z would not improve this bound in an essential way.

4. The onia of supersymmetry

4.1. Bound states of scalar quarks

If supersymmetric partners of quarks and gluons exist with masses in a range accessible in the near future, we expect a large variety of non-relativistic colour-singlet bound states. An efficient production mechanism of spin-1/2 states, for example $(Q\bar{Q})$ mesons, is not

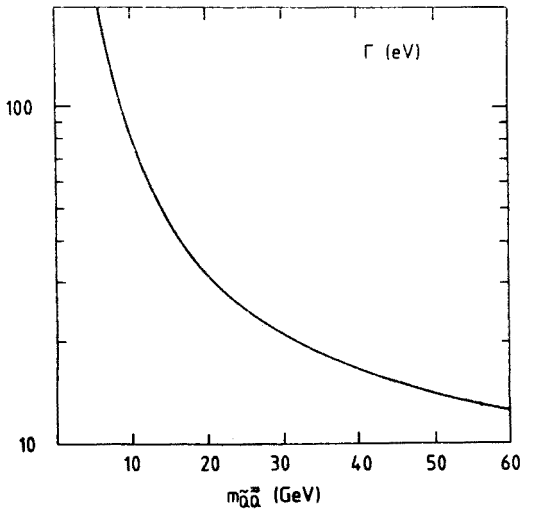

Fig. 20. Squarkonium decay rate into e^+e^-, calculated for potential T

easily conceivable. However, we may imagine the production of squarkonium[10] $(\tilde{Q}\bar{\tilde{Q}})$ states in e^+e^- annihilation [38, 39]. Their quantum numbers are given through

$$J = L, \quad P = C = (-1)^L. \tag{4.1}$$

Thus only P-states are accessible in e^+e^- annihilation. Production and annihilation rates of non-relativistic P-states are proportional to the derivative of the wave function at the origin. Compared with S-state rates, they are thus of order v^2/c^2, which implies a sizeable suppression of decays of heavy P-states. In Fig. 20 we show the partial rate

$$\Gamma[(\tilde{Q}\bar{\tilde{Q}}) \underset{\gamma}{\to} e^+e^-] = 24\alpha^2 e_Q^2 \frac{R'^2}{M^4} \tag{4.2}$$

[10] For a more detailed discussion of scalar-quark bound states, see Ref. [38].

with wave functions calculated for the potential T described in subsection 2.2. Evidently there is little hope of observing resonant production of squarkonia in e^+e^- annihilation. This result could have been guessed also from the slow rise of open squark production $\sim \beta^3$, using local duality. Note that the additional factor β which appears in the amplitude for scalar-quark production at threshold corresponds exactly to the derivative in front of the wave function for resonant squarkonium production.

4.2. Gluino-gluino bound states [40–43]

Systems which might be more easily accessible in e^+e^- experiments are gluino-gluino bound states, which have also been baptized gluino balls, glue-ballons, or gluinonia. Since present experiments do not (yet?) exclude the existence of relatively light gluinos (see subsection 2.1), the properties of these states have to be studied over a wide range of masses.

The requirement of totally antisymmetric wave functions for two identical Majorana particles allows only bound states of positive charge conjugation. We thus obtain the quantum numbers [40–44]

$$P = -(-1)^L, \quad C = 1. \tag{4.3}$$

Colour-singlet configurations (symmetric colour wave function!) admit only states with $L+S$ = even, and we thus expect as lowest-lying states 0^{-+} and 0^{++}, 1^{++}, 2^{++}. In the following we are mainly interested in gluinos, which are sufficiently heavy, so that a description in terms of a non-relativistic bound-state model is adequate ($m_{\tilde{g}} \gtrsim$ 2–3 GeV) or that at least the constituent picture is applicable ($m_{\tilde{g}} \gtrsim 1$ GeV). The short-distance part of the potential between colour octet gluinos in a colour singlet configuration is related to the quarkonium potential through

$$V_{\tilde{g}\tilde{g}} = \tfrac{9}{4} V_{Q\bar{Q}}. \tag{4.4}$$

The long-distance part will be qualitatively different, since the potential does not rise indefinitely, even in the absence of light quarks. However, because of the factor 9/4 which relates gluino and quark potentials, massive gluinos will be confined to small values of r where Eq. (4.4) is adequate. For our phenomenological analysis we extend this relation to arbitrary r.

Two gluinos may also combine into colour octet configurations [44] with a symmetric or an antisymmetric colour wave function. Now $L+S$ are constrained to be even or odd, depending on the symmetry of the colour wave function. Equation (4.3), however, is still valid. The potential is still attractive, but with a different normalization [44]

$$V^8_{\tilde{g}\tilde{g}} = \tfrac{9}{8} V_{Q\bar{Q}}. \tag{4.5}$$

We can thus envisage a situation where extremely heavy gluons are tightly bound into a colour octet state with a radius far smaller than the typical confinement distance. This bound state is then combined with a gluon into a colour singlet configuration. The study of such states would yield extremely valuable information on QCD dynamics [43]. However, their wave function at the origin is far smaller than the one of colour singlet states and so

are their production rates in all processes. We will therefore limit the following discussion to the colour singlet combinations.

The excitation energies of the lowest-lying bound states are shown in Fig. 21a (from Ref. [42]) calculated for Richardson's potential (R) and another one (T) which behaves somewhat more softly towards the origin (see subsection 2.2). Their excitation and binding

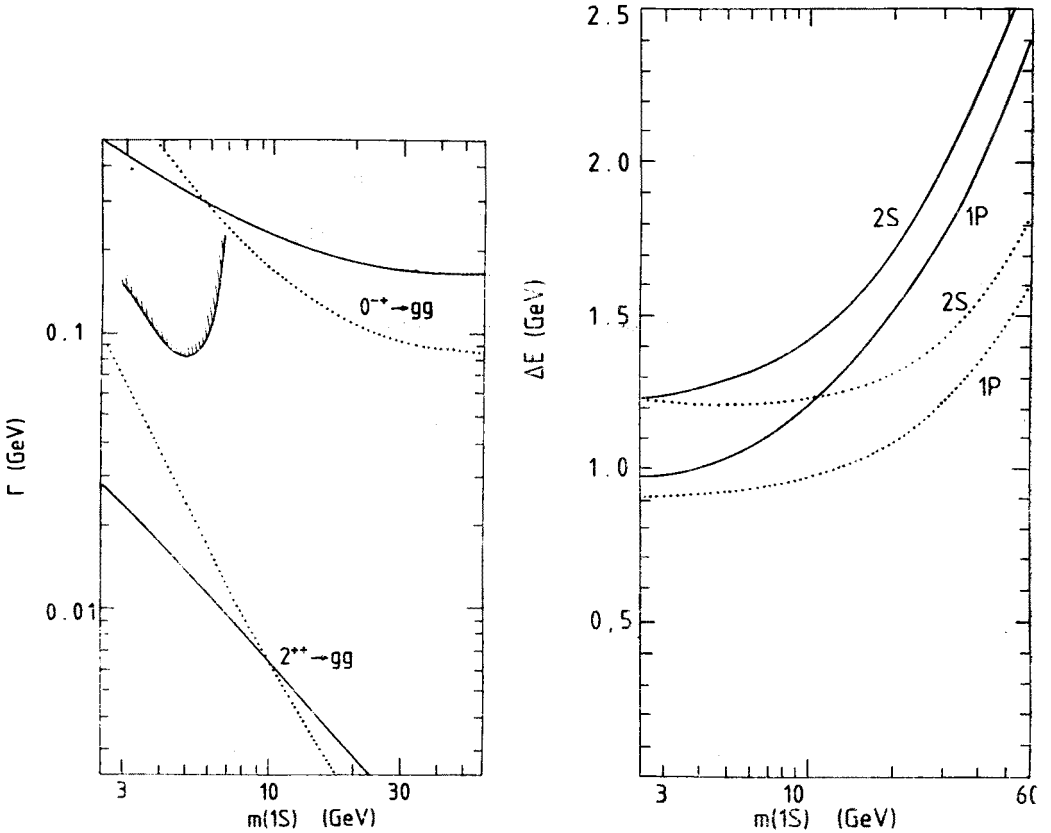

Fig. 21 a) Excitation energies $\Delta E = M - M(1S)$ of the lowest-lying gluino balls. Solid line V_R, dotted line V_T. b) Decay rates for $^1S_0$ and $^3P_2$ states as calculated for the two potentials (from Ref. [42]). The shaded curve indicates pseudoscalar decay rates, which are already excluded by the upper limits of radiative Υ decays from the CUSB Collaboration as discussed in the text

energies are far larger than those of quarkonia with the same mass, and their radii are smaller; thus they would provide otherwise inaccessible information on the short-distance part of the potential.

On the other hand, since we are probing deeply into an unknown region, the predictions are relatively sensitive towards the choice of the potential.

The dominant decay modes of the lowest-lying states are those into two gluons (for

0^{-+}, 0^{++}, and 2^{++}) and into $gq\bar{q}$ for 1^{++}. The evaluation of the corresponding rates is completely analogous to the corresponding quarkonium calculation. All decay rates are enhanced by a large colour factor,

$$\tfrac{1}{2}\left[\frac{C_2(A)/\sqrt{8}}{C_2(F)/\sqrt{3}}\right]^2 = \tfrac{27}{4}, \tag{4.6}$$

where the factor 1/2 is due to the Majorana property of gluinos. We thus find

$$\Gamma(0^{-+} \to gg) = \tfrac{27}{4}\tfrac{8}{3}\alpha_s^2 \frac{R(0)^2}{m(\tilde{g}\tilde{g})^2},$$

$$\Gamma(2^{++} \to gg) = \tfrac{27}{4}\tfrac{128}{5}\alpha_s^2 \frac{R'(0)^2}{m(\tilde{g}\tilde{g})^2},$$

$$\Gamma(0^{++}):\Gamma(1^{++}):\Gamma(2^{++}) = 15:\sim 1.5:4. \tag{4.7}$$

The same colour factor 27/4 appears also in the evaluation of all exclusive decay rates, if the annihilation proceeds through two intermediate gluons. The branching ratios can

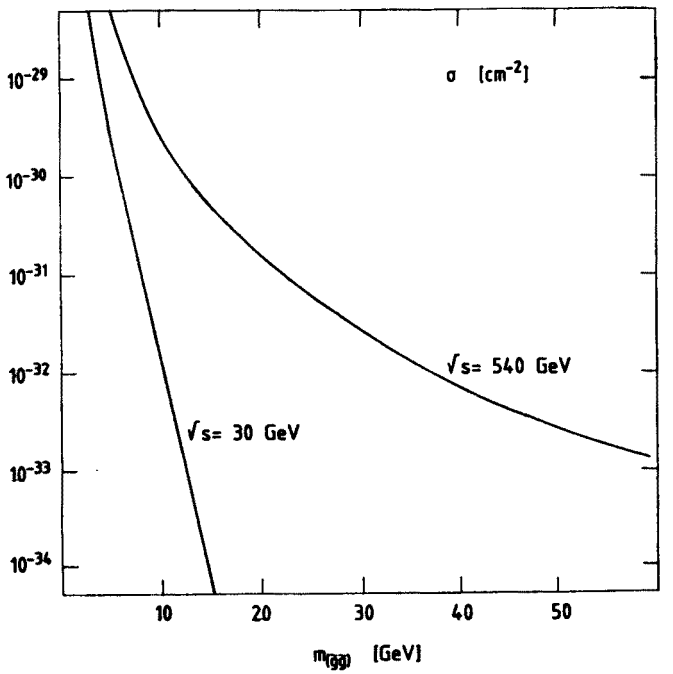

Fig. 22. Cross-section for production of pseudoscalar gluino balls in pp (or $p\bar{p}$) collisions (using V_R) (from Ref. [42])

thus be read off directly from the corresponding quarkonium calculation. Identification of gluino balls through these tiny channels looks rather hopeless.

As shown in Fig. 21b, the large wave function at the origin leads to decay rates which are typically two orders of magnitude larger than the corresponding quarkonium rates.

From these extremely large decay rates into gluons, we can expect sizeable production rates in hadronic collisions through gluon fusion. Indeed, remarkably large cross-sections can be found (Fig. 22). However, it seems to be a rather difficult task to identify these states, with their dominant hadronic multiparticle decay mode, amongst the background from conventional hadronic collisions.

Another, far more promising, reaction will be exclusive radiative quarkonium decays $^3S_1 \to \gamma + (\tilde{g}\tilde{g})$, which can proceed through a two-gluon intermediate state (Fig. 23a). The experimental signature would be a photon of fixed energy recoiling against an hadronic

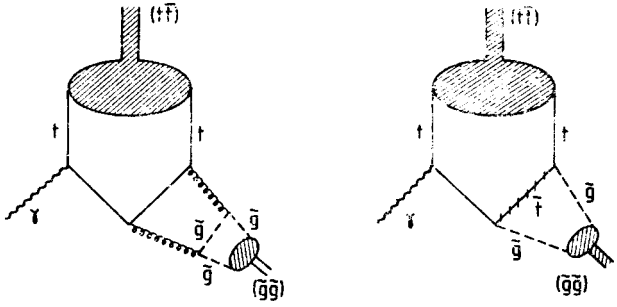

Fig. 23. Feynman diagrams for gluino ball production in quarkonium decays a) through virtual gluons, b) through squark exchange

system. (Note that gluino balls decay into two-gluon jets such that no missing energy is expected and the final state looks just like the one from conventional radiative decays $S_1 \to \gamma + g + g$). Considering the relatively large binding energy and the high threshold for open gluino production, resonance production would be kinematically strongly favoured in Υ decays if the gluino mass were below $\sim$ 5 GeV. Using earlier calculations for exclusive radiative decays into quarkonium pseudoscalar [45] and P-state [46] resonances, the rates for the corresponding decays into $(\tilde{g}\tilde{g})$ states are easily predicted [41–43]

$$\frac{\Gamma(^3S_1(Q\bar{Q}) \to \gamma + {}^1S_0(\tilde{g}\tilde{g}))}{\Gamma(^3S_1(Q\bar{Q}) \xrightarrow{}_{\gamma} e^+e^-)} = \frac{\alpha_s^2}{9\pi^2\alpha}\frac{m}{M^2}\Gamma(^1S_0 \to gg)x|\hat{H}^{PS}(x)|^2$$

$$\frac{\Gamma(^3S_1(Q\bar{Q}) \to \gamma + {}^3P_J(\tilde{g}\tilde{g}))}{\Gamma(^3S_1(Q\bar{Q}) \xrightarrow{}_{\gamma} e^+e^-)} = \frac{5\alpha_s^2}{18\pi^2\alpha}\frac{m}{M^2}\Gamma(^3P_2 \to gg)x\sum_J |\hat{H}_i^J|^2, \tag{4.8}$$

where

$$x = 1 - m^2/M^2, \quad m = m(\tilde{g}\tilde{g}), \quad M = M(Q\bar{Q}),$$

$$\hat{H}^{PS} = \frac{4}{x}\left\{\mathscr{L}_2(1-2x) - \mathscr{L}_2(1) - \frac{x}{1-2x}\ln 2x\right.$$

$$\left. - \frac{1-x}{2-x}[2\mathscr{L}_2(1-x) - 2\mathscr{L}_2(1) + \tfrac{1}{2}\ln^2(1-x)]\right\} + i\pi\frac{4}{x}\frac{1-x}{2-x}\ln(1-x).$$

The more complicated analytical results for the amplitudes $\hat{H}_i^J$ for P-states are given in Ref. [46]. The branching ratios for Υ decays and for a fictitious 60 GeV toponium state are shown in Figs. 24 and 25. We use $\mathrm{Br}(\Upsilon \to e^+e^-) = 3\%$, $\mathrm{Br}[(t\bar{t}) \to e^+e^-] = 10\%$, and the Richardson potential. Remarkably enough our prediction for Υ decays is already in conflict with the experimental upper limits for $\mathrm{Br}(\Upsilon \to \gamma + \text{narrow resonance})$, which is roughly 0.3×10^{-3} in the mass region between 2 and 7 GeV [47], and which was originally established as a result of the search for Higgs particles by the CUSB Collaboration (Fig. 26). The experimental upper limit on the branching ratio can be converted into an upper limit on $\Gamma[^1S_0(\tilde{g}\tilde{g}) \to gg]$, which is also shown in Fig. 21b. Considering the uncertainty in the

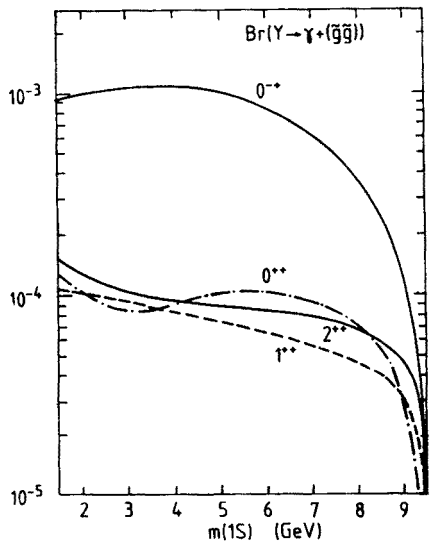

Fig. 24

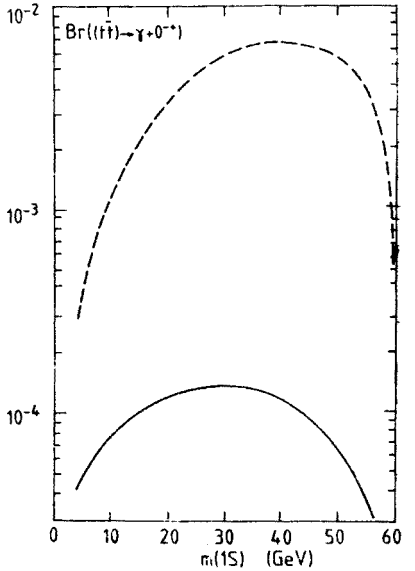

Fig. 25

Fig. 24. Branching ratios for Υ decays into 0^{-+}, 0^{++}, 1^{++}, and 2^{++} gluino balls as a function of $m_{\tilde{g}\tilde{g}}$ ($V = V^R$)
Fig. 25. Branching ratio for a 60 GeV toponium into a pseudoscalar gluino ball as a function of $m_{\tilde{g}\tilde{g}}$. Solid line: through virtual gluons; dashed line: through squark exchange under the assumptions specified in the text

choice of α_s and in the predictions of the colour octet potential, together with the preliminary nature of the data, it would be premature to already firmly exclude gluino bound states in this mass range. However, a moderate improvement of these limits would be sufficient to prove or disprove the existence of gluino balls with masses up to 8 GeV (corresponding to a bare gluino mass of $\sim$ 5 GeV).

The CUSB Collaboration was looking for a narrow resonance. The theoretically calculated width of the pseudoscalar, however, is comparable to the experimental mass resolution. If this mass resolution is smaller than the natural line width, the rate on top of the resonance is predicted independently of the potential, since the production rate and the height of the Breit-Wigner distribution are proportional to the square of the wave

function and its inverse, respectively. The photon rate on top of the resonance as a function of $x = 1-m^2/M^2$ is then given by

$$\frac{1}{\Gamma_{\text{tot}}}\frac{d\Gamma}{dx}\,(^3S_1 \to \gamma+(\tilde{g}\tilde{g})) = \text{Br}\,(^3S_1 \underset{\gamma}{\to} e^+e^-)\,\frac{\alpha_s^2}{9\pi^3\alpha}\,x$$

$$\times\{|\hat{H}^{\text{PS}}|^2; \tfrac{2}{3}\,|\hat{H}^{\text{S}}|^2; 6.7\sum_i |\hat{H}^{\text{A}}|^2; \tfrac{5}{2}\sum_i |\hat{H}^{\text{T}}|^2 \qquad (4.9)$$

and is shown in Fig. 27.

For the pseudoscalar case, the rate on top of the resonance would only be a factor of ~ 3 smaller than the background from γgg decays.

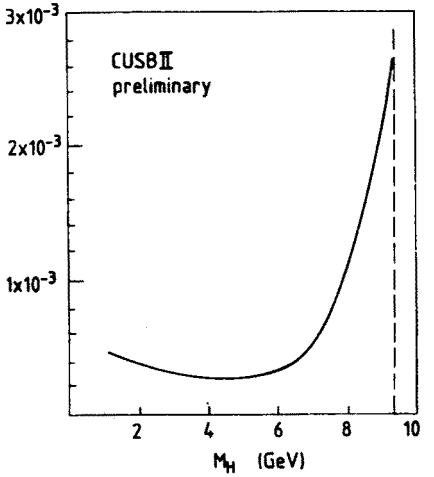

Fig. 26. Upper limits on decays of Υ into a photon plus narrow resonance as a function of resonance mass (from the CUSB Collaboration, Ref. [47])

If gluinos are relatively light, the non-relativistic model is subject to some doubt. However, a suitable generalization of the model [48] still allows prediction of the rates for decays into light mesons, e.g. η, η'. In this case the corresponding rate is no longer given by the wave function at the origin, but on the light cone. The dominant contribution, however, is still determined by the matrix element of a local operator, namely the divergence of the axial current $\langle qq|\partial^\mu \psi_q \gamma_\mu \gamma_5 \psi_q|0\rangle$ which appears instead of $R(0)$. This result can again be directly translated from quarks to gluinos. For a light ($m_{\tilde{g}\tilde{g}} \ll M$) pseudoscalar gluino ball, we find

$$\text{Br}(^3S_1 \to \gamma+(\tilde{g}\tilde{g})) = \text{Br}\,(^3S_1 \to e^+e^-)\,\frac{\alpha_s^4}{\alpha}\,\frac{2}{\pi}\left(\frac{\pi^2}{4}-\ln 2\right)^2 |\langle 0|\bar{\psi}_{\tilde{g}}\delta\gamma_5\psi_{\tilde{g}}|0^{-+}\rangle|^2. \qquad (4.10)$$

In principle the matrix element of ∂A could be evaluated in lattice calculations or through QCD sum rules to estimate the production rate of relatively light gluino balls in J/ψ decays.

Presumably this would then allow light gluinos ($m_{\tilde{g}\tilde{g}} \lesssim 2$ GeV) to be excluded, using a completely different method from that used for beam-dump experiments.

Our results for radiative decays are obviously independent of the mass of scalar quarks. Whilst this is certainly an advantage in the case of Υ decays, it might no longer be true

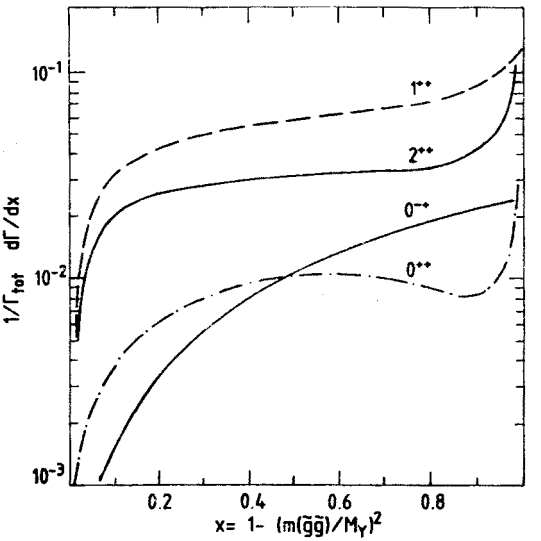

Fig. 27. Photon rate on top of the peak in the photon spectrum expected for a detector with good mass resolution [$< \Gamma_{\tilde{g}\tilde{g}}$]

for toponium decays. There, gluino ball production through s-top exchange (Fig. 23b), which is of order α_s^2, could play the dominant role. The decay rate for this mechanism[11] is given by [41]

$$\frac{\Gamma(^3S_1 \to \gamma + (\tilde{g}\tilde{g}))}{\Gamma(^3S_1 \to e^+e^-)} = \frac{64}{81\alpha} \frac{m(\tilde{g}\tilde{g})}{M^3} \Gamma((\tilde{g}\tilde{g}) \to gg) \left(\frac{m_t}{m_{\tilde{t}}}\right)^4 \left(1 - \frac{m(\tilde{g}\tilde{g})^2}{M^2}\right), \tag{4.11}$$

where $\tilde{m}_R = \tilde{m}_L = \tilde{m}$ has been assumed. In the general case the factor $1/\tilde{m}^4$ has to be replaced as follows:

$$\frac{1}{\tilde{m}^4} \to \left(\frac{1}{m_R^2} + \frac{1}{m_L^2}\right)^2 \tfrac{1}{4} + \left(\frac{1}{m_R^2} - \frac{1}{m_L^2}\right)^2 \tfrac{1}{4}. \tag{4.12}$$

In Fig. 24b we have shown the potentially expected branching ratio for $M_V = 60$ GeV. It is now more uncertain and depends not only on the unknown short-distance part of the potential but also on the mass of the scalar quark. We assumed $V = V$(Richardson) and the optimistic mass assignment $\tilde{m}_R = \tilde{m}_L = m_t$. For an 80 GeV toponium the branching ratio is reduced by a factor of roughly 1/3 owing to the increasing total width, and another

[11] It is assumed that one of the two contributing mechanisms dominates, which allows us to ignore interference effects.

factor of $\sim 9/16$ because of the $1/M^2$ dependence. Although these rates are larger than the gluon-mediated ones, only a dedicated effort would allow us to detect these states and study their properties. However, the prize would be truly rewarding.

I am indebted to S. Güsken, S. Ono, K. H. Streng and P. Zerwas for their collaboration on various aspects of quarkonium physics. Helpful discussions with W. Buchmüller, A. Martin and L. Sehgal are gratefully acknowledged.

I would also like to express my appreciation of the friendly and stimulating atmosphere in which the Zakopane School took place, and to thank the organizers for their hospitality.

Last but not least, I would like to thank K. Wakley, M.-S. Vascotto and M. Veyrat of the Documentation Department, for their magnificent help in preparing this manuscript.

APPENDIX

In this Appendix we present the derivation of the decay rates of quarkonium P-states and Z into a pair of Goldstone fermions, as discussed in subsection 3.4. The results for 0^{++}, 1^{++}, and Z decays are new; our rate for 2^{++} agrees with the formula given by Nachtmann and Wirbel [36].

All decay rates are deduced from the amplitude

$$\mathfrak{A} = \langle \lambda(p_1)\lambda(p_2)\, |i\kappa\bar{\psi}\gamma^\nu\partial^\mu\psi|0\rangle\, \langle 0|T_{\mu\nu}|R\rangle. \tag{A.1}$$

The first factor is antisymmetric in 1 and 2. Using the Majorana representation for the spinors corresponding to λ ($v^* = u$!) it can be written as

$$-\kappa(\bar{u}(p_2)\gamma^\nu p_1^\mu v(p_1) - \bar{u}(p_1)\gamma^\nu p_2^\mu v(p_2)) = -\kappa\bar{u}(p_2)\gamma^\nu(p_1-p_2)^\mu v(p_1). \tag{A.2}$$

For scalar, axial vector, and tensor resonances R, the form of the second factor, i.e. the matrix element of the canonical energy momentum tensor, is uniquely fixed

$$\langle 0|T_{\mu\nu}|R\rangle = \begin{cases} c_0 M^3(g_{\mu\nu} - P_\mu P_\nu/M^2) \\ c_1 M^3 \varepsilon_{\mu\nu\alpha\beta}\varepsilon^\alpha P^\beta \\ c_2 M^3 \varepsilon_{\mu\nu} \end{cases} \tag{A.3}$$

Here P and M denote the four-momentum and mass of the resonance, and $\varepsilon_\mu(\varepsilon_{\mu\nu})$ its polarization vector (tensor). The dimensionless constants c_i depend on the bound state and will be calculated. The corresponding matrix element for pseudoscalars vanishes owing to parity conservation. Also for vector states the decay is impossible, as long as parity is conserved. If parity is violated, as in Z decays discussed below, the relevant matrix element is of the same form as the one of the axial vector. Equations (A.2) and (A.3) lead to the following amplitudes and decay rates:

$$\begin{aligned} \mathfrak{A}_0 &= \kappa c_0 2m_\lambda M^3 \bar{u}(p_2)v(p_1), \\ \mathfrak{A}_1 &= -i\kappa c_1 M^4 \bar{u}(p_2)\not{\varepsilon}\gamma_5 v(p_1), \\ \mathfrak{A}_2 &= \kappa c_2 M^3 \varepsilon_{\mu\nu}\bar{u}(p_2)\gamma^\mu(p_1-p_2)^\nu v(p_1), \end{aligned} \tag{A.4}$$

$$\Gamma_J = \frac{1}{(2J+1)} \frac{M}{4\pi} \kappa^2 M^8 |c_J|^2 \left(1 - \frac{4m_\lambda^2}{M^2}\right)^{3/2} \begin{cases} m_\lambda^2/M^2 \\ \frac{1}{2} \\ \left(\frac{1}{4} + \frac{2}{3} \frac{m_\lambda^2}{M^2}\right) \end{cases} \tag{A.5}$$

It remains to evaluate the constants c_J.

For heavy quarkonia we make use of the weak binding approximation. For "free" quarks of momenta q_1 and q_2 the relevant matrix element reads

$$\langle 0|T^{\mu\nu}|\mathrm{Q}, \bar{\mathrm{Q}}\rangle = \bar{v}(q_1)\gamma^\mu \tfrac{1}{2}(q_1 - q_2)^\nu u(q_2). \tag{A.6}$$

To evaluate the corresponding matrix element for bound-state decays we use the general formalism of Ref. [49] for S- and P-wave annihilation. The expansion of the free quark amplitude $\bar{u}Ou$ in the relative momentum $(q_1 - q_2)/2$ up to linear terms

$$\bar{v}Ou = \bar{v}O(0)u + \tfrac{1}{2}(q_1 - q_2)^\alpha \bar{v}\hat{O}_\alpha u \tag{A.7}$$

is particularly simple in our case:

$$O(0) = 0; \quad \hat{O}_\alpha = \gamma^\mu g^\nu{}_\alpha. \tag{A.8}$$

This can be inserted directly in Eqs. (8a) to (8c) of Ref. [49]. Taking a factor of $\sqrt{3}$ from colour into account, one arrives at

$$c_J = \sqrt{\frac{3}{4\pi M^5}} R'(0) \begin{cases} 2 \\ \sqrt{6} \\ \sqrt{12} \end{cases} \tag{A.9}$$

and finally at Eq. (3.8).

The decay of Z into two Goldstone fermions proceeds through the parity-violating amplitude depicted in Fig. 19. The contribution from one colour triplet, weak isospin doublet, (t, b) with masses $m_t = m$, $m_b = 0$ to $\langle 0|T_{\mu\nu}|\mathrm{Z}\rangle$, which is logarithmically divergent, is given by

$$\langle 0|T_{\mu\nu}|R\rangle = -3g_A \int \frac{d^4q}{(2\pi)^4} \left\{ \mathrm{Tr}\left(-iE^\alpha \gamma_\alpha \gamma_5 \frac{i\left(\not{q} + \frac{\not{P}}{2} + m\right)}{\left(q + \frac{P}{2}\right)^2 - m^2} \right.\right.$$

$$\left.\left. \times \gamma_\mu i q_\nu \frac{i\left(\not{q} - \frac{\not{P}}{2} + m\right)}{\left(q - \frac{P}{2}\right)^2 - m^2} \right) - \mathrm{Tr}\,(\ldots)_{m=0} \right\}$$

$$= 3g_A 4i\varepsilon_{\alpha\beta\mu\delta} E^\alpha P^\beta \int \frac{d^4q}{(2\pi)^4} \left(\frac{q_\nu q_\delta}{\left[\left(q + \frac{P}{2}\right)^2 - m^2\right]\left[\left(q - \frac{P}{2}\right)^2 - m^2\right]} \right) - (\ldots)_{m=0}$$

$$= g_A c_Z M_Z^3 \varepsilon_{\alpha\beta\mu\nu} E^\alpha P^\beta, \tag{A.10}$$

where

$$c_Z = \frac{4i}{M_Z^2}\int \frac{d^4q}{(2\pi)^4} \frac{(q^2-(qP)^2/M_Z^2)}{\left[\left(q+\frac{P}{2}\right)^2-m^2\right]\left[\left(q-\frac{P}{2}\right)^2-m^2\right]} - (\ldots)_{m=0}. \tag{A.11}$$

The evaluation of the decay rate is essentially given by Eq. (A.5); it remains to perform the loop integral. The absorptive part is of course finite. The quadratic divergence of the dispersive part cancels. The logarithmic divergence is regularized by a cut-off Λ. For c_Z we obtain

$$c_Z = \tfrac{3}{2}\, i \int_{-1}^{1} dz \int_{\Lambda} \frac{d^4q}{(2\pi)^4} \frac{q^2}{M_Z^2} \left\{ \frac{1}{\left[q^2+\frac{P^2}{4}(1-z^2)-m^2\right]} - (\ldots)_{m=0} \right\},$$

which leads to our final result.

REFERENCES

[1] P. Schacht, Proc. 22nd Int. Conf on High-Energy Physics, Leipzig 1984, eds. A. Meyer and E. Wieczorek, p. 196.
[2] G. Arnison et al., (UA1 Collaboration), *Phys. Lett.* **147B**, 493 (1984).
[3] C. Quigg, J. L. Rosner, *Phys. Rep.* **56**, 167 (1979).
[4] H. Grosse, A. Martin, *Phys. Rep.* **60**, 341 (1980).
[5] H. Krasemann, S. Ono, *Nucl. Phys.* **B154**, 283 (1979).
[6] W. Buchmüller, G. Grunberg, S.-H. H. Tye, *Phys. Rev. Lett.* **45**, 103 and **45**, 587 (E) (1980); W. Buchmüller, S.-H. H. Tye, *Phys. Rev.* **D24**, 132 (1981).
[7] K. Koller et al., *Nucl. Phys.* **B193**, 61 (1981) and **B206**, 273 (1982).
[8] J. Ellis, M. K. Gaillard, CERN 76-18 (1976).
[9] K. Fujikawa, *Prog. Theor. Phys.* **61**, 1186 (1979).
[10] J. H. Kühn, Lectures given at at the 20th Cracow School of Theoretical Physics, Zakopane 1980 [*Acta Phys. Pol.* **B12**, 347 (1981)].
[11] I. Y. Bigi, H. Krasemann, *Z. Phys.* **C7**, 127 (1981).
[12] L. Sehgal, P. Zerwas, *Nucl. Phys.* **B183**, 417 (1981).
[13] J. H. Kühn, K. H. Streng, *Nucl. Phys.* **B198**, 71 (1982).
[14] L. Sehgal, Aachen preprint PITHA 83-9, Europhysics Study Conference on Electroweak Effects at High Energies, Erice, 1983 (to be published).
[15] J. H. Kühn, S. Ono, *Z. Phys.* **C21**, 395 (1984); *Erratum* **C24**, 404 (1984).
[16] J. H. Kühn, Lectures given at the 21st Int. Universitätswochen für Kernphysik, Schladming 1982 [*Acta Phys. Austriaca Suppl.* XXIV, 203 (1982)].
[17] M. Peskin, Stanford preprint SLAC-PUB-3273 (1983).
[18] W. Buchmüller, preprint CERN TH. 3938/84 (1984).
[19] I. Y. Bigi, J. H. Kühn, H. Schneider, Munich preprint MPI-PAE/PTh. 28/78 (1978).
[20] R. Koniuk et al., *Phys. Rev.* **D17**, 2915 (1978).
[21] R. Budny, *Phys. Rev.* **D20**, 2763 (1979).
[22] J. H. Kühn, F. Wagner, *Nucl. Phys.* **B236**, 16 (1984).
[23] LEP Design Report, Vol. II, CERN-LEP-84-01 (1984).
[24] F. M. Renard, *Z. Phys.* **C1**, 225 (1979).
[25a] J. H. Kühn, P. M. Zerwas, *Phys. Lett.* **154B**, 448 (1985).

[25b] S. Güsken, J. H. Kühn, P. M. Zerwas, *Phys. Lett.* **155B**, 185 (1985).
[26] J. L. Richardson, *Phys. Lett.* **82B**, 272 (1979).
[27] J. Kaplan, J. H. Kühn, *Phys. Lett.* **78B**, 252 (1978).
[28a] B. Campbell et al., *Nucl. Phys.* **B198**, 1 (1982).
[28b] G. Köpp, J. H. Kühn, P. M. Zerwas, *Phys. Lett.* **153B**, 315 (1985).
[29] E. Reya, P. P. Roy, *Phys. Lett.* **141B**, 442 (1984) and *Phys. Rev. Lett.* **53**, 881 (1984); J. Ellis, H. Kowalski, *Nucl. Phys.* **B246**, 189 (1984) and *Phys. Lett.* **142B**, 441 (1984).
[30] A. De Rujula, R. Petronzio, preprint CERN TH. 4070/84; V. Barger et al., *Phys. Rev. Lett.* **53**, 641 (1984).
[31] J. Ellis, S. Rudaz, *Phys. Lett.* **128B**, 248 (1983).
[32] B. Campbell et al., *Phys. Lett.* **131B**, 213 (1983).
[33] J. H. Kühn, *Phys. Lett.* **141B**, 433 (1984).
[34] W. Y. Keung, *Phys. Rev.* **D28**, 1129 (1983) [E. **D29**, 1544 (1984)].
[35] J. Wess, in *Quantum Theory of Particles and Fields* (Birthday volume dedicated to Jan Lopuszanski, eds. B. Jancewicz and J. Lukierski), World Scientific Publishers, Singapore 1983.
[36] O. Nachtmann, M. Wirbel, *Z. Phys.* **C23**, 85 (1984).
[37] O. Nachtmann et al., *Z. Phys.* **C23**, 199 (1984).
[38] C. Nappi, *Phys. Rev.* **D25**, 84 (1982).
[39] H. Krasemann, *LEP Study Group*, unpublished.
[40] D. Nanopoulos et al., *Phys. Lett.* **137B**, 363 (1984).
[41] W. Y. Keung, A. Khare, *Phys. Rev.* **D29**, 2657 (1984).
[42] J. H. Kühn, S. Ono, *Phys. Lett.* **142B**, 436 (1984).
[43] S. Ono, Tokyo preprint UT 438 (1984).
[44] T. Goldman, H. Haber, Los Alamos preprint LA-UR 84-634 (to be published in *Physica D*).
[45] B. Guberina, J. H. Kühn, *Lett. Nuovo Cimento* **32**, 295 (1981).
[46] J. Körner, J. H. Kühn, M. Krammer, H. Schneider, *Nucl. Phys.* **B229**, 115 (1983), and references therein.
[47] P. Franzini (CUSB Collaboration), results presented at the fifth Moriond Workshop on Heavy Quarks, Flavour Mixing, and CP Violation, La Plagne 1985.
[48] J. H. Kühn, *Phys. Lett.* **127B**, 257 (1983).
[49] J. H. Kühn, J. Kaplan, E. G. O. Safiani, *Nucl. Phys.* **157B**, 125 (1979).